2012-12-17

Quantum Storage and Retrieval of Light by Sweeping the Atomic Frequency

Kaviani, Hamidreza

UNIVERSITY OF CALGARY

Quantum Storage and Retrieval of Light by Sweeping the Atomic Frequency

by

Hamidreza Kaviani

A THESIS

SUBMITTED TO THE FACULTY OF GRADUATE STUDIES

IN PARTIAL FULFILLMENT OF THE REQUIREMENTS FOR THE

DEGREE OF MASTER OF SCIENCE

DEPARTMENT OF PHYSICS AND ASTRONOMY

CALGARY, ALBERTA

December, 2012

UNIVERSITY OF CALGARY

FACULTY OF GRADUATE STUDIES

The undersigned certify that they have read, and recommend to the Faculty of Graduate Studies for acceptance, a thesis entitled "Quantum Storage and Retrieval of Light by Sweeping the Atomic Frequency" submitted by Hamidreza Kaviani in partial fulfillment of the requirements for the degree of MASTER OF SCIENCE.

Supervisor, Dr. Christoph Simon
Department of Physics and Astronomy

Dr. David Hobill
Department of Physics and Astronomy

Dr. Alex Lvovsky
Department of Physics and Astronomy

Dr. John Nielsen
Department of Electrical Engineering

Date

Abstract

We propose and analyze a quantum memory protocol based on dynamically changing the resonance frequency of an ensemble of two-level atoms. By sweeping the atomic frequency in an adiabatic fashion, photons are reversibly transferred into atomic coherences. We present a polaritonic description for this type of storage, which shares lots of similarities with Electromagnetically Induced Transparency (EIT) based quantum memories. On the other hand this memory is linked to the Gradient Echo Memory(GEM) quantum memory in the co-moving frame due to the effective spatial gradient that pulses experience in the medium. As a result the proposed protocol forms a bridge between two well-known protocols for quantum memory, which is conceptually a matter of interest in the field of quantum memories. We also present a numerical analysis of this memory protocol and discuss various conditions that have to be fulfilled for desirable memory performance.

Acknowledgments

I would like to express my sincere gratitude to my supervisor Dr. Christoph Simon who not only guided my project but also familiarized me with the strange world of quantum physics. He gave me the confidence and ideas to push my research to what I thought was out of my reach. I would like to thank my supervisory committee members Dr. David Hobill and Dr. Alex Lvovsky for fruitful discussions. I would also like to thank Dr. Paul Barclay and Dr. Alex Lvovsky for introducing me to quantum optics and photonics by providing great courses.

Special thanks go to my colleague and more importantly my friend Khabat Heshami for sharing his knowledge patiently with me. He almost played the role of my co-supervisor by continuously discussing the details and technical aspects of the project. Many thanks go to Mohammad Khazali. Without his help, I couldn't have established the mathematical tools used in this project. I would like to thank Ehsan Zahedinejad for giving me help with the numerical simulations and Adam D'Souza for editing the text of the thesis. I would also like to thank Farid Ghobadi who was my best friend and colleague during my masters. I enjoyed inspiring scientific and non-scientific discussions with him during my stay in Calgary. I am grateful to my friend and past colleague, Sadegh Raeisi, to help me to settle down in Calgary. I never forget his friendly support when I was settling for the first time in a foreign country.

Most importantly, I would like to thank my parents, Shahla Ghafourian and Javad Kaviani for all their sacrifices for me in order to stand where I am. At last but not the least I would like to thank my kind wife, Nasrin Mostafavi Pak. Words cannot describe how she gives me endless love and hope in my entire life.

Table of Contents

List of Figures and Illustrations

Chapter 1

Introduction

Storage and retrieval of photons on-demand is essential in quantum information processing tasks such as implementation of single photon sources, long-distance quantum communication and distributed quantum computing [1][6][7]. Quantum memory can be achieved by coherent control of the atom-photon interaction. Some protocols for quantum memory introduce a control beam in a three-level atomic configuration (e.g. Electrically Induced Transparency (EIT) [8] and Raman scheme [9][10][11]) to manipulate the interaction between the signal pulse and the atoms. Other protocols use the phenomenon photon echo[12][13] to achieve controlled atom-photon interaction. In this type of memory the atom-photon interaction is controlled in a more indirect way by a dephasing-rephasing process owing to the inhomogeneous broadening of the medium. Atomic Frequency Comb memory (AFC) [5], Controlled Reversible Inhomogeneous Broadening memory (CRIB)[14] and Gradient Echo Memory (GEM)[15] are examples of this type of protocols.

Recently it has been shown that some of these protocols can be emulated by dynamically changing certain characteristics of an ensemble of two-level atoms. For instance, it has been shown that by dynamically controlling the transition dipole moment of an ensemble of two-level atoms, one can emulate Raman-type quantum memories[16]. More recently it has been shown that changing the refractive index of the host medium of two-level atoms is equivalent to GEM memory[17].

Here we study another way of manipulation of the atom-photon interaction, namely by sweeping the resonance frequency. When the light is in resonance with the atoms, the interaction is on and when the detuning is large compared to the bandwidth of the pulse, the interaction is off. The energy levels of the two-level atoms can be changed by applying a magnetic or electric field depending on the system.

We demonstrate that this protocol can be described in terms of polaritons similar to dark-state

polaritons in EIT [2]. By changing the detuning, the pulse slows down and is stored in atomic coherences. Changing the detuning plays the role of changing the control field in EIT. However there are also difference between the two polaritonic pictures, in particular, in our protocol the pulse doesn't shrink at the beginning of the medium, in contrast with EIT.

Intuitively this protocol is similar to the GEM protocol for the regime in which pulses are short compared to the medium. While we change the detuning in time during the propagation of the pulse through the medium, the pulse effectively sees the spatial gradient in the energy levels of the atoms, and atomic coherence becomes dephased.

In chapter 2 we review the theory and experiments of quantum storage based on EIT and derive the dark state polaritons. In chapter 3 we review photon echo quantum memories including CRIB, GEM and AFC. We also discuss about experimental implementations of these protocols. In chapter 4 we describe the main focus of this thesis which is quantum memory with sweeping atomic frequency. We present the polaritonic picture and numerical analysis for this memory in this chapter. In chapter 5 we show the link between GEM and atomic frequency sweep memory analytically by going to the co-moving frame. We also compare these two protocol by providing numerical analysis. Lastly, the concolution and final remarks are discussed in the chapter 6.

Chapter 2

Quantum Memory Based on Dark-State Polariton in Electromagnetically Induced Transparency (EIT)

Electromagnetically Induced Transparency (EIT) is a nonlinear phenomenon in atoms with a three-energy-level configuration usually with Λ structure (Figure.2.1). In the absence of a strong control field, the weak signal field is absorbed by the transition, with which it is resonant.

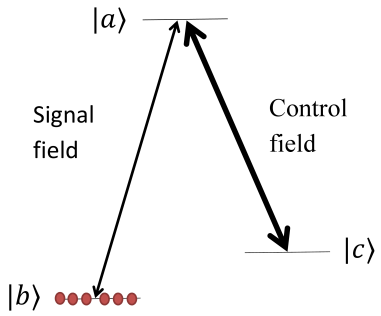

Figure 2.1: Energy levels of atoms with a Λ-structure. Atoms are initially in the ground state b. The signal quantum field and strong control field are on resonance with b-a and c-a transitions respectively.

In the presence of a control field, destructive quantum interference between the probability of transitions a-b and a-c, causes the atoms to stay in the ground state b, and the field is not absorbed by the medium. This phenomenon, where the control field makes the opaque medium transparent is called EIT. Therefore EIT opens a transparent window at the resonance frequency with width proportional to the intensity of the control field (Fig.2.2). According to the Kramers-Kronig relations, followed by a change in the refractive index of the medium.

This change in refractive index results in a reduction of the group velocity by a factor proportional to the inverse of the control field intensity. Experiments have shown that light can be slowed

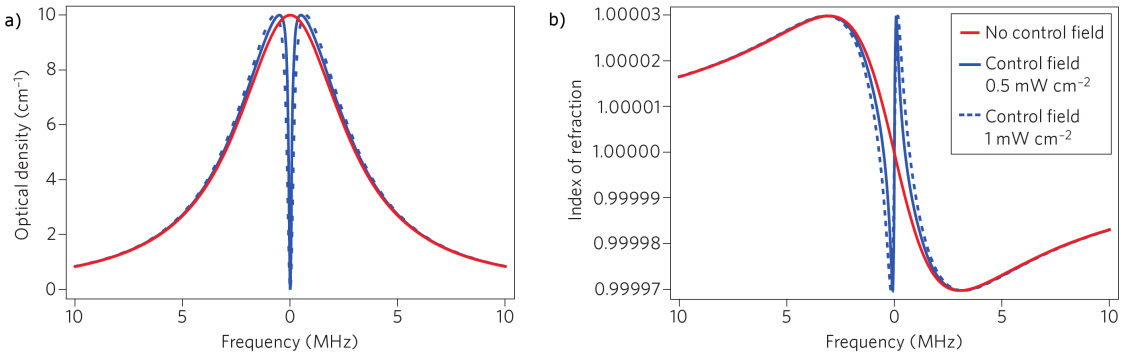

Figure 2.2: Absorption profile (a) and refractive index profile (b) of the medium without (red) and with (blue) control field. It can also be seen that how transparency window changes with change in intensity of control field (dashed line). The atomic parameter used for this plot corresponds to cloud of ultra cold rubidium atoms. Image courtesy of ref.[1]

by seven orders of magnitude [18].

It has been shown [2] that there is a form-stable excitation associated with the propagation of pulses in such a medium, called "dark-state polariton", which is a superposition of light and atomic polarization. While the dark-state polariton is preserved during the propagation, photonic and atomic contributions in dark states can be manipulated by adiabatic changes of the control field. Also the group velocity is directly related to the ratio of atomic and photonic contributions in the dark state polariton.

As a result, by adiabatically changing the control field, one can slow down the light and transfer the photonic state to an atomic state, and by reversing the process retrieve the photonic pulse. Thus, the dark-state polariton in EIT is a suitable candidate for a quantum memory.

We consider an ensemble of Λ-type three-level atoms. Figure 2.1 shows the energy configuration of the atoms with two metastable ground states (b,c) and one excited state(a) . $\hat{E}$ is the signal which is the quantum field that we aim to store and $\Omega(t)$ is the time dependent Rabi frequency of the control field. We assume that both the control field and the signal are in resonance with their corresponding transitions.

Propagation of the light inside the atomic medium is governed by Maxwell's equations, which leads to the following wave equation

$$\frac{\partial^2 E}{\partial z^2} - \frac{1}{c^2}\frac{\partial^2 E}{\partial t^2} = \frac{1}{c^2 \varepsilon_0}\frac{\partial^2 P}{\partial t^2} \tag{2.1}$$

where E and P are the electric field and polarization of the atoms respectively. Here, without loss of generality, we consider a one-dimensional system for the sake of simplicity. We also use the slowly-varying approximation by introducing slowly-varying amplitudes $\mathscr{E}(z,t)$ and $\mathscr{P}(z,t)$

$$E(z,t) = \mathscr{E}(z,t)e^{i(k_0 z - \omega_0 t)} + c.c. \tag{2.2}$$

$$P(z,t) = \mathscr{P}(z,t)e^{i(k_0 z - \omega_0 t)} + c.c. \tag{2.3}$$

Here, k_0 and ω_0 are the central wave vector and frequency respectively. Under slowly-varying conditions;

$$\begin{pmatrix} \partial_z \\ \partial_t \end{pmatrix} (\mathscr{E}, \mathscr{P}) \ll \begin{pmatrix} k_0 \\ \omega_0 \end{pmatrix} (\mathscr{E}, \mathscr{P}) \tag{2.4}$$

the wave equation of 2.1 is simplified to

$$(\frac{\partial}{\partial z} + \frac{k_0}{\omega_0}\frac{\partial}{\partial t})\mathscr{E}(z,t) = \frac{i\omega_0^2}{2\varepsilon_0 k_0 c^2}\mathscr{P}(z,t) \tag{2.5}$$

A quantum field can be described by the dimensionless annihilation and creation operators [19]

$$\hat{E}(z,t) = \int d\omega \hat{a}_\omega(t)e^{ikz} + c.c. \tag{2.6}$$

where $\hat{a}_\omega$ is annihilation operator of photon with frequency of ω. We also can write the polarization of one atom as

$$P^j(t) = d\hat{\sigma}^j_{ba} + c.c. \tag{2.7}$$

where $\hat{\sigma}_{ba}^{j} = |b_j\rangle\langle a_j|$ is the matrix element ofthe polarization of the j^{th} atom, and $d = d_{ab} = d_{ba} = e\langle b|\vec{r}|a\rangle$ is the dipole moment of the atom. Eq.(2.3) together with Eq.(2.7) leads us to the expression for the slowly-varying collective polarization;

$$\mathscr{P}(z,t) = de^{-i(k_0 z-\omega_0 t)}\frac{1}{N_z}\sum_{j=1}^{N_z}\hat{\sigma}_{ba}^{j}n(z) \tag{2.8}$$

where $n(z) = \frac{N}{V}$ is the atomic density and $d\frac{1}{N_z}\sum_{j=1}^{N_z}\hat{\sigma}_{ba}^{j}$ is the average polarization in the tiny slice but microscopic volume in the z position which contains N_z atoms.

Now we define the collective operator as follows:

$$\hat{\sigma}_{\alpha\beta}(z,t) = \frac{1}{N_z}\sum_{j=1}^{N_z}\hat{\sigma}_{\alpha\beta}^{j}e^{i\omega_{\alpha\beta}(t-\frac{z}{c})} \tag{2.9}$$

By introducing the collective operators, Eqs.(2.5)(2.8) lead to the field equation in terms of the collective operator,

$$(c\frac{\partial}{\partial z}+\frac{\partial}{\partial t})\hat{\mathscr{E}}(z,t) = igN\hat{\sigma}_{ba} \tag{2.10}$$

where $g = \frac{d\cdot\varepsilon_k\hat{\varepsilon}}{\hbar}$ is the atom-field coupling constant, $\varepsilon_k = \sqrt{\frac{\hbar\omega_0}{2\varepsilon_0 V}}$ is the electrical field per volume V and N is the number of atoms in the medium.

The atomic evolution in the interaction picture is given by the Heisenberg equation

$$\frac{\partial}{\partial t}\hat{\sigma}_{\alpha\beta} = -\gamma_{\alpha\beta}\hat{\sigma}_{\alpha\beta}+\frac{i}{\hbar}[\hat{V},\hat{\sigma}_{\alpha\beta}]+F_{\alpha\beta} \tag{2.11}$$

where $\gamma_{\alpha\beta}$ is the decay rate of the polarization matrix element $\hat{\sigma}_{\alpha\beta}$, $F_{\alpha\beta}$ is the Langevin noise operator, and $\hat{V}$ is the interaction Hamiltonian which governs the interaction between light and atoms in free space,

$$\hat{V} = -\sum_{j=1}^{N}(\hbar g\int\hat{a}_\omega e^{ikz_j}\hat{\sigma}_{ab}^{j}e^{i\omega_{ab}(t-\frac{z}{c})}d\omega+\hbar\Omega\hat{\sigma}_{ac}^{j}e^{i\omega_{ac}(t-\frac{z}{c})})+H.c. \tag{2.12}$$

Here, $\Omega(t)$ is the Rabi frequency of the control field which is applied to a-c transition (Fig.2.1).

By substituting the interaction Hamiltonian 2.12 into the Heisenberg equation 2.11 and taking commutators, we end up with a set of equations of motion for the atomic operators

$$\frac{\partial}{\partial t}\hat{\sigma}_{aa} = -\gamma_{aa}\hat{\sigma}_{aa} - ig(\mathscr{E}^{\dagger}\hat{\sigma}_{ba} - H.c.) - i\Omega(\hat{\sigma}_{ca} - \hat{\sigma}_{ac}) + \hat{F}_{aa} \tag{2.13}$$

$$\frac{\partial}{\partial t}\hat{\sigma}_{bb} = -\gamma_{bb}\hat{\sigma}_{bb} - ig(\mathscr{E}\hat{\sigma}_{ab} - H.c.) + \hat{F}_{bb} \tag{2.14}$$

$$\frac{\partial}{\partial t}\hat{\sigma}_{cc} = -\gamma_{cc}\hat{\sigma}_{cc} - i\Omega(\hat{\sigma}_{ac} - \hat{\sigma}_{ca}) + \hat{F}_{cc} \tag{2.15}$$

$$\frac{\partial}{\partial t}\hat{\sigma}_{ba} = -\gamma_{ba}\hat{\sigma}_{ba} - ig\mathscr{E}(\hat{\sigma}_{aa} - \hat{\sigma}_{bb}) + i\Omega\hat{\sigma}_{bc+}\hat{F}_{ba} \tag{2.16}$$

$$\frac{\partial}{\partial t}\hat{\sigma}_{ca} = -\gamma_{ca}\hat{\sigma}_{ca} + ig\mathscr{E}\hat{\sigma}_{cb} - i\Omega(\hat{\sigma}_{aa} - \hat{\sigma}_{cc}) + \hat{F}_{ca} \tag{2.17}$$

$$\frac{\partial}{\partial t}\hat{\sigma}_{bc} = -\gamma_{bc}\hat{\sigma}_{bc} - ig\mathscr{E}\hat{\sigma}_{ac} + i\Omega\hat{\sigma}_{ba} + \hat{F}_{bc} \tag{2.18}$$

In the above equations we assume for simplicity that the Rabi frequency is real. In the weak-field condition that the number of photons is much smaller than the number of atoms, we can assume that the atomic population remains mostly in the ground state b ($\sigma_{bb} = 1$). Therefore, we can neglect the population of states a and c ($\sigma_{aa} = \sigma_{cc} = 0$). Moreover in the weak-field regime, atomic equations can be treated perturbatively in $\hat{\mathscr{E}}$. To first order in $\hat{\mathscr{E}}$, we have

$$\hat{\sigma}_{ba} = -\frac{i}{\Omega}\frac{\partial}{\partial t}\hat{\sigma}_{bc} \tag{2.19}$$

$$\sigma_{bc} = -\frac{g\hat{\mathscr{E}}}{\Omega} - \frac{i}{\Omega}[(\frac{\partial}{\partial t} + \gamma_{ba})(-\frac{i}{\Omega}\frac{\partial}{\partial t}\sigma_{bc})] + \hat{F}_{ba} \tag{2.20}$$

Considering the adiabatic conditions [20], one can introduce normalized time $\widetilde{t}$ with time scale T ($\widetilde{t} = \frac{t}{T}$). With that, Eq.(2.20) to lowest order in $\frac{1}{T}$ is given by

$$\sigma_{bc} = -\frac{g\hat{\mathscr{E}}}{\Omega} \tag{2.21}$$

It is worth mentioning that $F_{\alpha\beta}$ is not the lowest order of $\frac{1}{T}$ due to the fact that $\langle F_x(t)F_y(t)\rangle$ $\delta(t-t') = \delta(\tilde{t}-\tilde{t}')/T$.

Plugging Eq.(2.19) into Eq.(2.10) yields the wave equation

$$(c\frac{\partial}{\partial z} + \frac{\partial}{\partial t})\mathscr{E}(z,t) = \frac{gN}{\Omega}\frac{\partial}{\partial t}\hat{\sigma}_{bc} \tag{2.22}$$

To make the equations symmetric in terms of the interaction coefficient, we apply the transformation ($\sigma_{bc} \to \sqrt{N}\sigma_{bc}$), giving

$$\sigma_{bc} = -\frac{g\sqrt{N}\hat{\mathscr{E}}}{\Omega} \tag{2.23}$$

$$(c\frac{\partial}{\partial z} + \frac{\partial}{\partial t})\mathscr{E}(z,t) = \frac{g\sqrt{N}}{\Omega}\frac{\partial}{\partial t}\hat{\sigma}_{bc} \tag{2.24}$$

Now we simplify the equation by introducing a new quantum field $\hat{\Psi}$ which is a mixture of field and atomic operators

$$\hat{\Psi}(z,t) = cos\theta\hat{\mathscr{E}}(z,t) + sin\theta\hat{\sigma}_{bc}(z,t) \tag{2.25}$$

By substituting Eqs.(2.23) and (2.25) into the field equation 2.24, we obtain

$$\begin{aligned} &\frac{\Omega}{\Omega\cos\theta - g\sqrt{N}\sin\theta}(c\frac{\partial}{\partial z} + \frac{\Omega^2 + g^2N}{\Omega^2}\frac{\partial}{\partial t})\hat{\Psi}(z,t) \\ &= -\{\frac{\dot{\Omega}}{\Omega\cos\theta - g\sqrt{N}\sin\theta} + \frac{\Omega^2 + g^2N}{\Omega}\frac{\partial}{\partial t}(\frac{1}{\Omega\cos\theta - g\sqrt{N}\sin\theta})\} \end{aligned} \tag{2.26}$$

One can choose $\sin\theta$ and $\cos\theta$ so as to have a non-dispersive quantum field, which results in the right-hand side of Eq.(2.26) being equal to zero:

$$\frac{\dot{\Omega}}{\Omega\cos\theta - g\sqrt{N}\sin\theta} + \frac{\Omega^2 + g^2N}{\Omega}\frac{\partial}{\partial t}\left(\frac{1}{\Omega\cos\theta - g\sqrt{N}\sin\theta}\right) = 0 \tag{2.27}$$

This leads to a relationship between $\sin\theta$ and $\cos\theta$

$$\Omega\cos\theta - g\sqrt{N}\sin\theta = \sqrt{\Omega^2 + g^2N} \tag{2.28}$$

Thus, together with the normalization condition ($\cos^2\theta + \sin^2\theta = 1$) yields

$$\cos\theta = \frac{\Omega(t)}{\sqrt{\Omega^2(t) + g^2N}} \tag{2.29}$$

$$\sin\theta = \frac{-g\sqrt{N}}{\sqrt{\Omega^2(t) + g^2N}} \tag{2.30}$$

Now we end up with the quantum field $\hat{\Psi}$ with field and atomic contributions given by $\cos\theta$ and $\sin\theta$ respectively, which satisfies the non-dispersive wave equation

$$\left(\frac{\partial}{\partial t} + c\cos^2\theta\frac{\partial}{\partial z}\right)\hat{\Psi}(z,t) = 0 \tag{2.31}$$

$\hat{\Psi}$ is the shape-preserving field whose group velocity is controlled by the control field. By changing the control field and thus θ from zero (which corresponds to strong control field compared to coupling) to $\frac{\pi}{2}$ (which corresponds to absence of control field), one can stop the light and map it onto the polarization of atoms. By turning on the control field again, light can be reconstructed from the atomic coherence and accelerated to the speed of light. Figure.(2.3) shows this reversible transferring of light to matter.

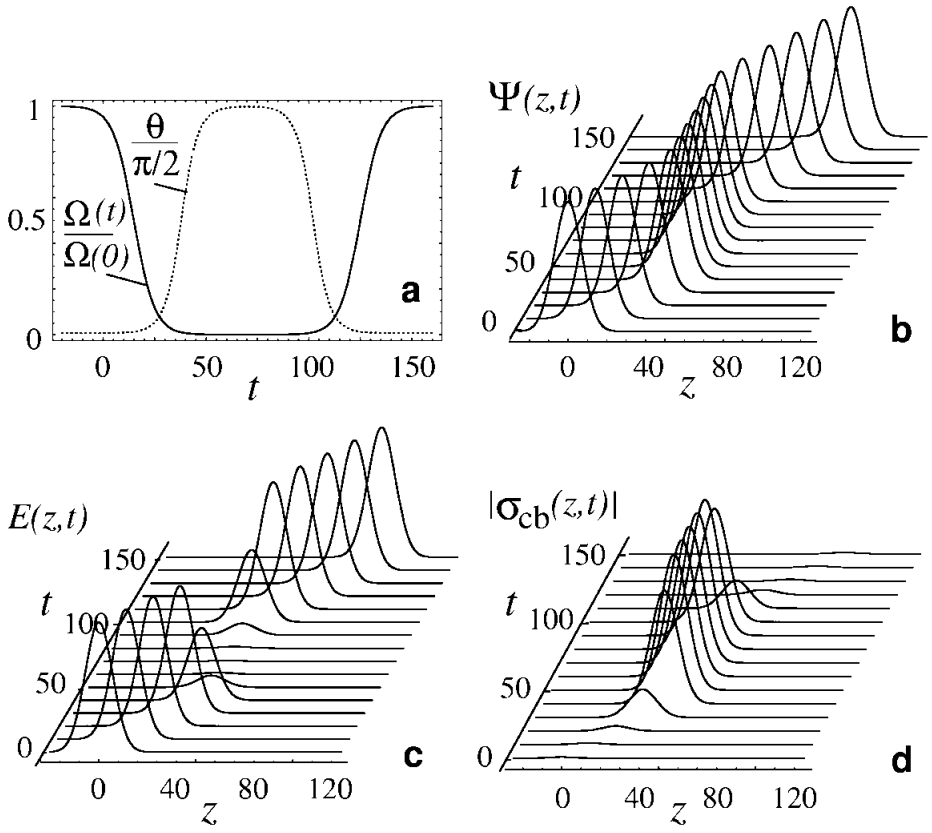

Figure 2.3: Propagation of dark-state polariton. The initial electric field is a Gaussian envelope $exp(-z/10)^2$. (a) The control field changes with time such that mixing angle θ changes between 0 and $\frac{\pi}{2}$ with the form $\cot\theta(t) = 100(1-0.5\tanh[0.1(t-15)]+0.5\tanh[0.1(t-125)])$. The polariton freely propagates through the medium (b) while (c) the electric field amplitude $|\langle\hat{E}\rangle|$ and (d) atomic coherence amplitude $|\langle\hat{\sigma}_{cb}\rangle|$ interconvert between each other. Axes are in arbitrary units, assuming c=1. Image courtesy of ref. [2]

In 2001, two groups demonstrated storage of classical light based on EIT. D.Phillips et al.[21] stored a $10-30\mu s$ optical pulse at a wavelength of 795 nm in a $4Cm$ atomic Rubidium vapor cell at temperature $70-90^\circ$ for up to $200\mu s$. C.Liu et al.[22] demonstrated storage of $5.70\mu s$ pulses in magnetically trapped sodium atoms cooled to 0.9 μK for up to 0.9 ms.

EIT-based memory can also be realized in solid media. The advantage of using solid media is to allow for longer storage time. Longdell et al.[23] stored light in $4mm$ long praseodymium-doped Y_2SiO_5 crystals with a storage time of more than one second. The disadvantage of using Ion-doped crystals is their low optical depth, which results in low efficiency. Due to inhomogeneous

broadening in such crystals, increasing the density of dopants only causes a broader absorption linewidth without increasing the optical depth. For example, in the afore mentioned experiment, the efficiency is of the order of 1%.

In 2005 T.Chanelière et al.[24] stored pulses at the single photon level in cold atomic clouds of Rb confined in magneto-optical traps (MOTs) with optical depth $d = 7$ for up to $15\mu s$, with an efficiency of 0.06%. In the same year, M.Eisaman et al.[25] demonstrated storage of a single photon with $0.5\mu s$ storage time and 10% efficiency in a $4.5cm$-long Rb vapor cell with optical depth around $d = 4$. The efficiency of storage based on EIT was improved to almost 50% with storage time of up to $400\mu s$ by I.Novikova et al.[26]. They achieved this memory efficiency by optimizing the shape of the input pulse in a Rubidium vapor cell with optical depth $d \approx 9$.

In 2008 J.Appel et al.[27] demonstrated storage of squeezed light in Rubidium vapor cell for up to $1\mu s$, which shows that EIT based quantum memories are compatible with continuous-variable quantum information protocols.

Chapter 3

Photon Echo Quantum Memory

EIT-based quantum memories suffer from an intrinsic trade off between the transparency window, which determines the permitted spectral bandwidth of the input pulse, and reduction in the group velocity of the pulse. As can be seen in Figure.(2.2) by widening the transparency window the slope of the refractive index decreases, which results in lesser reduction in group velocity. This fact limits the spectral bandwidth of the input pulse, and makes multimode storage of pulses very difficult. Photon echo quantum memory protocols are proposed to get around this problem. Photon echo is the optical analogue to the well-known spin echo in nuclear magnetic resonance(NMR) discovered by Hahn in 1950 [28]. Photon echo was demonstrated by Kopvil'em et al.[12] and Kurnit et al.[13] independently in 1963 and 1964 respectively. Two decades later the idea was extended to store classical data by Elyutin et al.[29] and Mosseberg et al.[30], and technique has been improved to store a data sequence of 1760 optical pulses[31].

Photon echo can be understood well in the Bloch sphere description of light-atom interaction. At first, all atoms are in the ground state, so the atomic state can be described by the vector along negative w. By applying $\frac{\pi}{2}$ pulse we rotate the vector to the u direction (Figure.3.1.a). Due to inhomogeneous broadening of the medium, each component of the atomic state rotates with a different frequency in the u-v plane and atomic states become dephased (Figure.3.b). At time τ, by applying π-pulse atomic states will be rotated by π around the v axis (Figure.3.c). Due to inversion of atomic states, after time τ, atoms rephase and form a macroscopic dipole and emit the first echo.

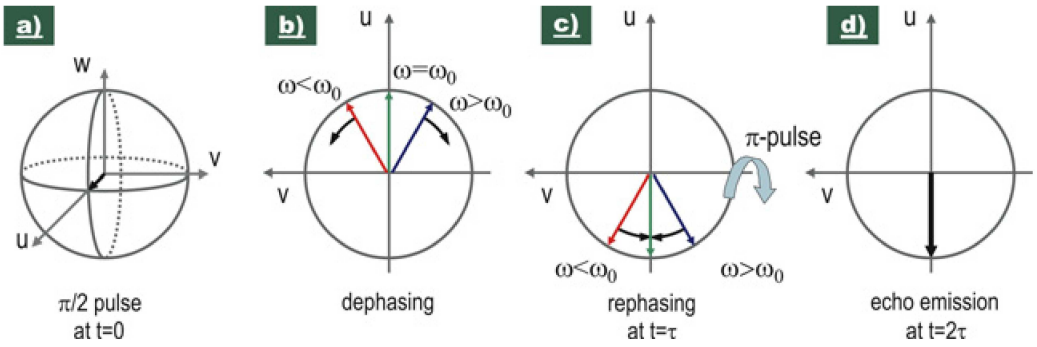

Figure 3.1: Evolution of the atomic state in the Bloch sphere in the two-pulse photon-echo process.(a) By applying $\frac{\pi}{2}$ pulse, the atomic state rotates from the ground state (negative w) to the u direction. (b) The atomic phase undergoes a dephasing process owing to inhomogeneous broadening. (c) At time $t = \tau$ π-pulse rotates all the vectors around the v axis. (d) At time $t = 2\tau$ all the vectors have rephased and form a macroscopic dipole, and the first echo is emitted. Image courtesy of ref.[3]

Although traditional photon echo has been successful in storing classical light, for storing single photons this protocol suffers from noise resulting from the applied π pulses. When we apply a π-pulse, we bring the atomic population into the excited state and it will cause noise and amplifying spontaneous emission due to the dipole-dipole interaction. This effect makes the conventional photon echo protocol inappropriate for storing single photons.[32]

Nevertheless this technique inspired the other protocols for storing pulses at single photon level. Consider an inhomogeneous ensemble of two-level atoms interacting with a single-photon pulse. After the absorption of the photon, since we don't know which atom absorbed the photon, the atomic state becomes the collective state

$$|\psi\rangle = \sum_{j=1}^{N} c_j e^{i\delta_j t} e^{-ikz_j} |g_1 ... e_j ... g_N\rangle \tag{3.1}$$

where $|g_1 ... e_j ... g_N\rangle$ is the state corresponding to all atoms in ground state except for the j^{th} atom, which absorbed the photon. k is the wave vector of the field and z_j is the position of the absorber atom. c_j is a probability amplitude which depends on the frequency and position of the j^{th} atom. δ_j is the detuning of the j^{th} atom with respect to the central frequency of the field. At first all atomic phases are in phase with the spatial atomic mode, but since detuning differs for each

atom, atoms become dephased with respect to the spatial mode, and re-emission of the photon is suppressed. All photon echo quantum memories use a procedure to rephase the atomic dipoles with the spatial mode to produce an echo at some later time. Based on the procedure that these protocols use for rephasing the atomic state, they can be classified into two categories: Controlled Reversible Inhomogeneous Broadening (CRIB) and Atomic Frequency Comb (AFC).

3.1 Controlled Reversible Inhomogeneous Broadening (CRIB)

This protocol uses spectral hole burning and controllable Stark shift from an electrical gradient to rephase and dephase the atomic state for the purpose of quantum memory.

The essence of this memory is the hidden time reversibility in the Maxwell-Bloch equations. The light is absorbed in the inhomogeneous broadening which is made using Stark shift. Time reversal of corresponding Maxwell-Bloch equations shows it is possible to convert the atomic excitation into a photonic excitation and retrieve the field. Reversing of the process apart from reversing the inhomogeneous broadening, requires an application of the phase matching operation, which is equivalent to applying a phase shift e^{-2ikz_j} to all atoms. This causes the forward collective atomic excitation (which was created during the absorption) to turn into a backward collective atomic excitation, leading to the backward-traveling output field.

Now we show rigorously the above mentioned time reversibility in the Maxwell-Bloch equations. We consider a two-level ensemble of atoms with ground state $|g\rangle$ and excited state $|e\rangle$. The electric field is in general composed of a backward and forward traveling component

$$E(z,t) = E_f(z,t)e^{ikz} + E_b(z,t)e^{-ikz} \tag{3.2}$$

Here for simplicity, we consider a one-dimensional propagation model. The pulse is detuned with respect to the inhomogeneously broadened atoms. $\Delta^j = \omega_0 - \omega_{eg}^j$ is the detuning of the j^{th} atom with respect to the central frequency of the pulse ω_0. Since we have a distribution of energy levels due to inhomogeneous broadening, we introduce $\rho(\Delta)$, which is the number of atoms with

detuning Δ compared to the central frequency of the pulse, such that $\int d\Delta\rho(\Delta) = N$. To describe the quantum properties of the medium, we introduce the collective operator for atoms with the same detuning with respect to the pulse

$$\sigma_{ij}(z,t;\Delta) = \frac{1}{N(\Delta,z)} \sum_{n=1}^{N(\Delta,z)} |i\rangle_{nn}\langle j| \tag{3.3}$$

Here, $|i\rangle$and $|j\rangle$ are either $|g\rangle$ or $|e\rangle$. $N(\Delta,z) = \rho(\Delta)d\Delta$ is the number of atoms with detuning Δin the position of z.

The Hamiltonian which describes such a system in the rotating wave approximation and in the rotating frame is given by

$$\mathscr{H} = \int_{-\infty}^{+\infty} d\Delta \frac{\rho(\Delta)}{L} \int_0^L dz[\hbar\Delta\sigma_{ee}(a,t;\Delta) - \hbar g E(z,t)\sigma_{eg}(z,t;\Delta) + H.c.] \tag{3.4}$$

where $g = \frac{d\cdot\varepsilon_k\hat{\varepsilon}}{\hbar}$ is the coupling constant between atom and photon, $d = d_{ge} = d_{eg} = e\langle e|\vec{r}|g\rangle$ is the dipole moment of the transition e-g and $\varepsilon = \sqrt{\frac{\hbar\omega_0}{2\varepsilon_0 V}}$ is the electric field per volume.

Similar to the electric field, the atomic coherence is composed of a backward and forward traveling components

$$\sigma_{ge}(z,t;\Delta) = \sigma_f(z,t;\Delta)e^{ikz} + \sigma_b(z,t;\Delta)_b(z,t)e^{-ikz} \tag{3.5}$$

In the weak field approximation, where we can assume that most of the population is in the ground state ($\sigma_{gg} = 1$), the equations of motion for both the forward and backward components of atomic coherence is given by the Heisenberg-Langevin equations and in slowly-varying amplitude approximation,

$$\frac{\partial}{\partial t}\sigma_f(z,t;\Delta) = -i\Delta\sigma_f(z,t;\Delta) + igE_f(z,t) \tag{3.6}$$

$$\frac{\partial}{\partial t}\sigma_b(z,t;\Delta) = -i\Delta\sigma_b(z,t;\Delta) + igE_b(z,t) \tag{3.7}$$

Here, since we are interested in time scales smaller than the decay time, we neglect the decay. The equation of motion for the forward and backward traveling components of the field in the slowly-varying amplitude approximation is given by

$$(\frac{\partial}{\partial t}+c\frac{\partial}{\partial z})E_f(z,t)=ig\int_{-\infty}^{+\infty}d\Delta\rho(\Delta)\sigma_f(z,t;\Delta) \tag{3.8}$$

$$(\frac{\partial}{\partial t}-c\frac{\partial}{\partial z})E_b(z,t)=ig\int_{-\infty}^{+\infty}d\Delta\rho(\Delta)\sigma_b(z,t;\Delta) \tag{3.9}$$

Due to linearity of the equations of motion, these equations can be used for the both classical and single photon wavefunction. For classical light, E_f and E_b are the classical fields and σ_f and σ_b are the atomic polarizations. Analogously, E_f, E_b, σ_f and σ_b can be interpreted as single photon wavefunctions and single excitation wavefunctions respectively for the quantum case.

This memory protocol can be understood by time symmetry analysis of the equations of motion. Time reversal can be accomplished via transformation

$$t\rightarrow -t \tag{3.10}$$

$$\Delta\rightarrow -\Delta \tag{3.11}$$

$$E_b\rightarrow -E_b \tag{3.12}$$

The last transformation is due to the fact that the signs of emitted and absorbed fields are opposite. By performing this transformation, the equations of motion for the backward component are converted to the equations of motion for the forward component of the atomic and photonic coherences. To retrieve the field in the backward direction, in addition to reversing the inhomogeneous broadening, the phase matching operation also needs to be performed on the atomic coherence, which is equivalent to applying a phase shift e^{-2ikz_j} to all atoms.

Time symmetry analysis shows that it is possible to store and retrieve the light with high efficiency and fidelity. Since the equations of motion are linear, we can solve the equations analytically and obtain the efficiency for this protocol. For the case of constant inhomogeneous broadening absorption line in the medium, in the regime where the frequency bandwidth of the pulse is smaller than the inhomogeneous broadening, and applying the phase matching operation so that the output pulse propagates in the backward direction, the output field reads as

$$E_b^{out}(0,t) = -(1-e^{-d})E_f^{in}(0,-t) \tag{3.13}$$

where $d = \alpha L = 2\pi\frac{g^2 NL}{\gamma c}$ is the effective optical depth and γ is the inhomogeneous broadening bandwidth . Under the same condition; when the phase matching operation is not performed and we read out the output from the forward direction, it can be shown that the output field is[14]

$$\widetilde{E}_f^{out}(L,\omega) = -de^{-\frac{d}{2}} sinc(\frac{\omega L}{c})\widetilde{E}_f^{in}(0,-\omega) \tag{3.14}$$

where $sinc(x) = \frac{sin(x)}{x}$. In the regime where the spectral bandwidth of the input pulse is smaller than $\frac{c}{L}$, which corresponds to pulses larger than the size of the medium, $sinc(\frac{\omega L}{c})$ can be treated as the delta function $\delta(\frac{\omega L}{c})$. With that, Eq.(3.14) in the time domain is reduced to

$$E_f^{out}(L,t) = -de^{-\frac{d}{2}} E_f^{in}(0,-t) \tag{3.15}$$

The memory efficiency, which is the probability of retrieving the pulse for both backward and forward read-out is shown in Figure3.2 in terms of the optical depth αL

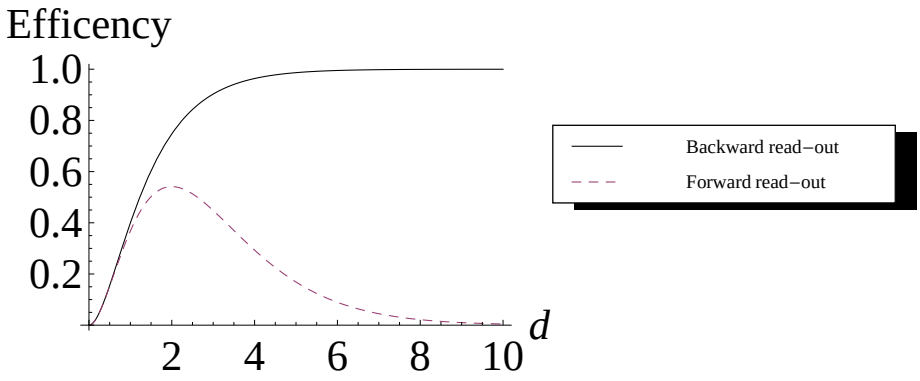

Figure 3.2: Efficiency in the CRIB protocol for forward (dashed red line) and backward readout (solid blue line)

For small optical depth, the both forward and backward readout behave quadratically with optical depth. However, in the forward readout due to the reabsorption of the pulse by the medium, the efficiency drops with increased optical depth, which is not the case for backward readout. This fact is due to the exponential dependence of the atomic coherence on the distance that the pulse travels in the medium. As a result, most of the atomic coherence is formed at the beginning of the medium. Therefore if we read out the light in the backward protocol we have less medium ahead of the propagating light, which results in less reabsorption compared to the forward protocol. Due to this fact the efficiency of forward readout is limited and the maximum efficiency is 54% at the optical depth $d = 2$.

3.1.1 Realization

The method of implementation of reversible inhomogeneous broadening depends on the system of interest. In atomic vapor with natural Doppler broadening CRIB can be achieved by using this fact that Doppler broadening changes sign when direction of propagation of light is reversed[33]. By applying the phase matching operation to the atomic coherence, one can invert the propagation of the light and consequently reverse the Doppler broadening. Complete reversal of the Doppler broadening requires the atoms to have constant velocity during the storage procedure. Thus, stor-

age time of this protocol is limited by the collision time of the atoms.

In solid state materials, there is natural inhomogeneous broadening due to the different position of the atoms in the crystal. This broadening can be controlled by narrowing the naturally broadened transition which can be achieved by optical pumping. Then, by applying an external field gradient, we reach again the broadened absorption line, due to Stark or Zeeman shift. This time, however, the broadening is reversible by reversing the external field.

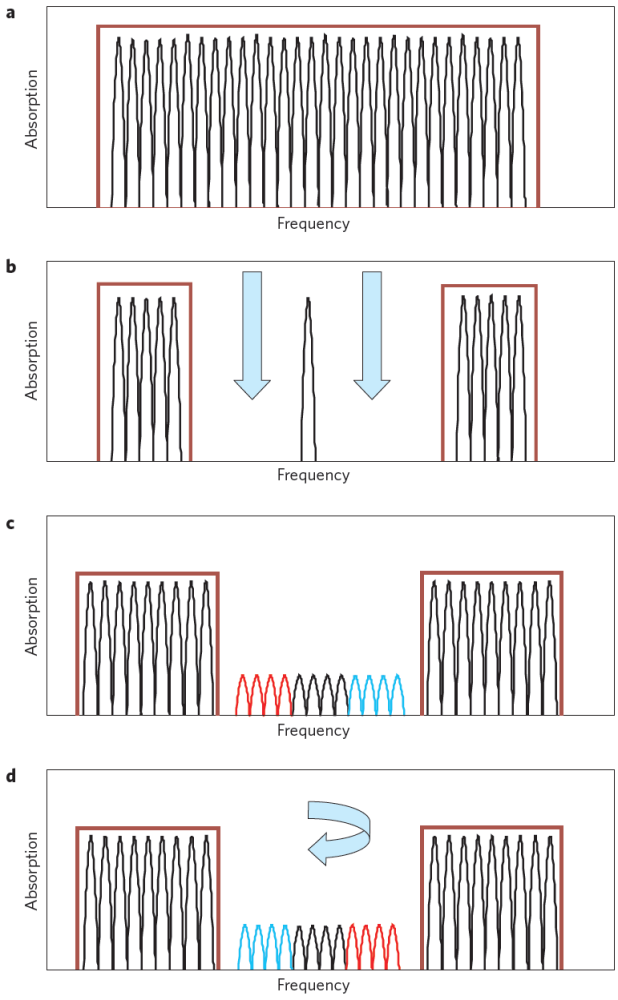

Figure 3.3: CRIB realizations steps. In step 1, by optical pumping, a narrow absorption line is created. In step 2, by using an external field, the isolated absorption line is broadened. In step 3, the incident photon is absorbed and undergoes a dephasing process. In step 4, by reversing the polarity of the field, the atomic coherence is rephased and the photon is emitted emit. Image courtesy of ref.[3]

The storage time is limited by the spectral width of the initial absorption line in the first prepara-

tion step of CRIB (Figure.3.1.1 .step2). As a result, narrowing the initial line increases the storage time. However it decreases the optical depth of the system due to optical pumping of more atoms, and consequently decreases memory efficiency. This problem can be solved by transferring the atomic population of the broadened excited state to another long-lived excited state, which allows one to start with a wider initial absorption line. This transfer can be achieved by using a π-pulse or using Raman transfer via an off-resonant control field that connects levels $|a\rangle$ and $|b\rangle$.

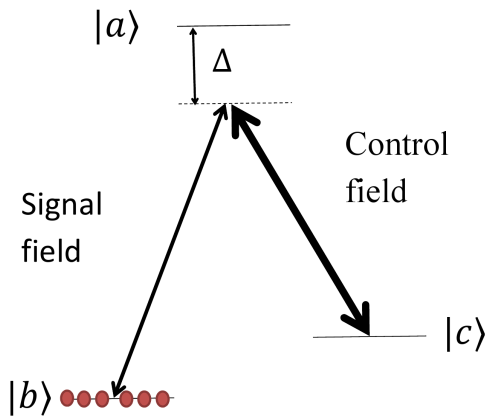

Figure 3.4: Off resonant transfer of the exited state to another metastable ground state

If the control field counterpropagates with respect to the signal field, it also applies the phase matching operation which is necessary for the retrieving pulse in the backward direction. The combination of Raman transfer and CRIB is often called Raman echo quantum memory.

3.1.2 Gradient echo memory(GEM)

As mentioned earlier, The efficiency of reading out the pulse in the forward direction, due to reabsorption of the echo pulses by the medium is limited to 54%. We can get around this problem by sorting the absorption frequencies through the optical path of the light which can be achieved by applying an external field gradient longitudinally rather than transversally. If the energy level of the atoms changes monotonically through the medium in the retrieval process (Figure.3.5.b) when we flip the polarity of external field, the echo from each part of the medium is not on resonance

with the rest of the medium. Thus it doesn't get reabsorbed by the medium. Therefore we don't have the problem of limited efficiency in the forward protocol in the GEM memory, in contrast with transverse CRIB. This variation of CRIB is often called gradient echo memory (GEM)

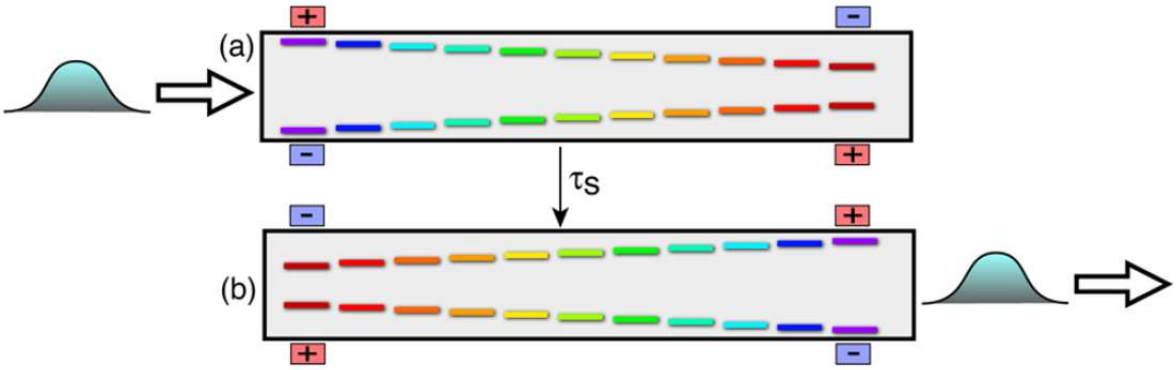

Figure 3.5: Schematic illustration of longitudinal CRIB also known as GEM. In contrast with transverse CRIB, atomic frequencies are ordered in space by applying a spatial linear gradient of an external field. (b) After time τ_s, by flipping the polarity of the field, the atomic coherence rephases and the input signal retrieved. Image courtesy of ref.[4]

In the GEM protocol, we assume a linear external electric field gradient through the propagation of light. This external field causes the detuning of the atoms and the light to depend on the longitudinal position of atoms in the medium. For analyzing such a system, we can use the Maxwell-Bloch equations Eqs.3.6 and 3.8 which we obtained for the forward component of the atomic coherence and field in CRIB. In the case of GEM the detuning of atoms depends linearly on their position, so we denote detuning as $\Delta(z) = -\chi z$, where χ is the slope of the change of detuning in the longitudinal coordinate (z). In addition, the density $\rho(\Delta)$ can be reduced to $N\delta(\Delta - \chi z)$. With these changes, Eqs.3.6 and 3.8 reduce to

$$\frac{\partial}{\partial t}\sigma(z,t) = -i\chi z\sigma(z,t) + igE(z,t) \tag{3.16}$$

$$(\frac{\partial}{\partial t} + c\frac{\partial}{\partial z})E(z,t) = igN\sigma(z,t) \tag{3.17}$$

By solving these equations, it can be shown that the efficiency of such a memory protocol in the regime where spectral bandwidth of the input pulse is smaller than the inhomogeneous broadening, is given by $\eta = (1 - e^{-d'})^2$ where $d' = 2\pi \frac{g^2 N}{c\chi}$ is the effective optical depth [15]. It is worth mentioning that this expression for efficiency can also be obtained by substituting χL for the inhomogeneous broadening bandwidth (γ) in equation 4.22, which is the solution of CRIB for the backward readout.

The first proof-of-principle realization of CRIB was performed in a $4mm$-long europium-doped Y_2SiO_5 crystal cooled to $4K$ [34]. The gradient of the electric field in this experiment was transverse to the propagation direction of the pulse and was implemented with four electrodes in a quadrapole configuration. Storage of a $3\mu s$ pulse with a decay time of $20\mu s$ was observed. Due to the low absorption of the medium (40% for the narrowed linewidth and 1% for the broadened linewidth) only between a 10^{-5} and 10^{-6} portion of the input pulse was retrieved. Most CRIB experiments have been performed in the version of GEM when the gradient of field is longitudinal, so the efficiency in the forward direction has no fundamental limit. The record to date for the GEM protocol at the single photon level is storing $2\mu s$ pulses for $3\mu s$ with efficiency 78% and fidelity as high as 99% in a Rubidium vapor cell with temperature higher than room temperature [35]. The GEM memory has also been implemented in a solid state medium. M.Hedges et al. [36] stored pulses with $0.6\mu s$ FWHM with a decay time of $3\mu s$ in a praseodymium-doped Y_2SiO_5 single crystal with an efficiency of up to 69% . In this experiment, the atoms are not transfered to another long-lived state for the reason that the atomic structure levels of this crystal do not allow isolated ground states to be exist.

3.2 Atomic Frequency Comb (AFC)

Another way of implementing a photon echo quantum memory is by creating a periodic structure absorption profile, which looks like a comb. This can be done by frequency-selectively transferring atomic population from $|g\rangle$ to an auxiliary metastable state $|aux\rangle$.

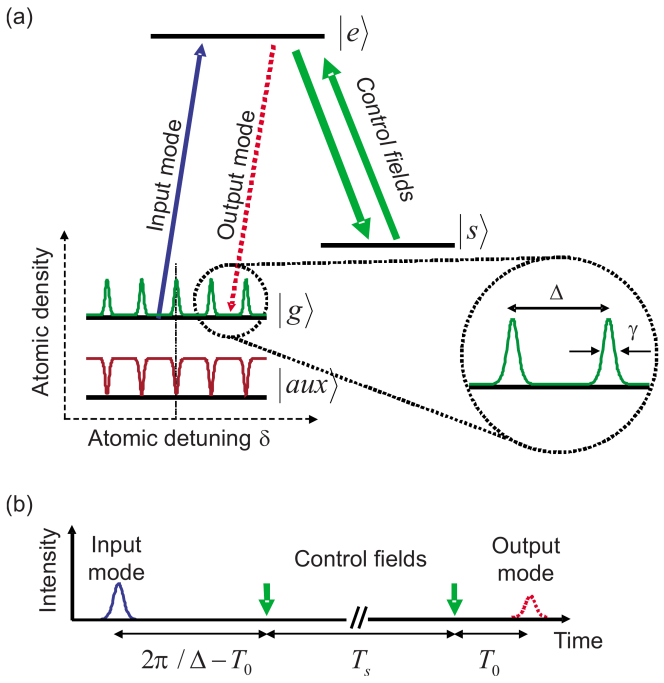

Figure 3.6: Illustration of AFC protocol. (a) AFC structure is tailored for the transition g-e by frequency-selective optical pumping of atoms to the auxiliary state $|aux\rangle$. The AfC teeth have a width of γ and are separated by Δ. A photon is absorbed by the g-e transition and dephases and then rephases after time $2\pi/\Delta$. Rephasing can be delayed by transferring the excited state to another ground state $|s\rangle$ which determines the storage time T_s (b). Image courtesy of ref.[5]

For storing the input field, which is in resonance with atomic transition, the spectral bandwidth of the input field γ_p has to be larger than the peak separation Δ. On the other hand it has to be smaller than the total width of AFC $\Gamma(\Delta \ll \gamma_p \ll \Gamma)$. Although the field is subjected to a narrow-peak absorption line, if the optical depth is large enough, the field can be absorbed by the medium. This fact can be explained by the Heisenberg energy-time uncertainty relation. During the absorption time, which is of the order of the time duration of the pulse($\frac{1}{\gamma_p}$), the transition has an uncertainty greater than γ_p. Therefore, if the spectral bandwidth of the pulse (γ_p) is larger than the peak separation (Δ), the input pulse will see a smooth spectral absorption linewidth which is an averaged version of the sharp AFC structure.

Here we consider storage of a single photon inside the medium. After absorption of a photon, since we don't know which atom absorbed the photon, the atomic state becomes a collective state

$$|\psi\rangle = \sum_{j=1}^{N} c_j e^{i\delta_j t} e^{-ikz_j} |g_1 ... e_j ... g_N\rangle \tag{3.18}$$

where $|g_1 ... e_j ... g_N\rangle$ corresponds to all atoms being in the ground state except the j^{th} atom, which absorbed the photon. k is the wave vector of the field and z_j is the position of the absorber atom. c_j is a probability amplitude that depends on the frequency and position of the j^{th} atom. δ_j is the detuning of the j^{th} atom with respect to the central frequency of the field. If we consider sharp distinct peaks with a peak separation of Δ, δ_j can be approximated by $\delta_j = m_j\Delta$, where m_j is an integer. At first, all components of the collective atomic coherence are in phase with the spatial mode k. However due to inhomogeneous broadening, each atomic component dephases with a different frequency in time. Owing to the periodic structure of the atomic frequencies with a periodicity of Δ, all components become in phase after a time $\frac{2\pi}{\Delta}$, which leads to the first echo in the direction of the wave vector. For on-demand readout and long storage time, we can transfer atomic population by applying a π-pulse from the excited state to the other spin ground state $|s\rangle$. As a result, the rephasing process will stop and there will be no echo. For the read-out process, we can transfer the atoms back to the excited state and let them rephase and produce an echo. The control field also can be used as a tool for determining the direction of readout. If we apply a counterpropagating control field with respect to the signal field, the output field is retrieved in the backward direction. If the control field copropagates with the signal, the output will be in the forward direction.

The Maxwell-Bloch equations for the AFC are similar to the equations of motion for CRIB Eqs.3.6-3.9, with the difference that in the AFC case, the atomic spectral distribution $\rho(\Delta)$ is described by a series of Gaussian functions with width $\widetilde{\gamma}$ and peak separation Δ, and total width Γ

$$\rho(\delta) = e^{-\frac{\delta^2}{2\Gamma^2}} \sum_{j=-\infty}^{\infty} e^{-\frac{(\delta - j\Delta)^2}{2\widetilde{\gamma}}} \tag{3.19}$$

For characterizing the comb structure, we introduce the AFC finesse F as $F = \frac{\Delta}{\gamma}$, where $\gamma = \sqrt{8ln2}\widetilde{\gamma}$ is the full width at half-maximum (FWHM). This quantity quantifies how well the peaks are separated.

Considering the AFC condition for the spectral bandwidth of the input pulse ($\Delta \ll \gamma_p \ll \Gamma$), and assuming that population transfer is performed perfectly and neglecting decoherence, it can be shown that the relationship between the output and input fields in the backward direction is given by [5]

$$E_b(z=0,t=\frac{2\pi}{\Delta}) = -E_f(z=0,t=0)e^{-i2\pi\frac{\Delta_0}{\Delta}}(1-e^{-\widetilde{d}})e^{-(\frac{1}{F^2})(\frac{\pi^2}{4\ln 2})} \tag{3.20}$$

The first factor is a global phase due to the offset between the central frequency of the AFC and the input pulse (Δ_0). The second factor represents the atom-photon interaction, where $\tilde{d} = \frac{d}{F}$ is the effective optical depth of the AFC. Effective optical depth is inversely proportional to finesse as expected, since for higher finesses (which corresponds to making the peaks sharper) we need to remove more atoms by means of optical pumping, which reduces optical depth. The third factor is due to dephasing owing to the finite width of the teeth. There are two competing factors in determining AFC efficiency in terms of finesse. By increasing finesse, on the one hand effective optical depth decreases, but on the other hand the efficiency increases due to having more distinct teeth. These facts determine to the optimum value for finesse. Fig.3.7 shows how efficiency varies as we change the finesse.

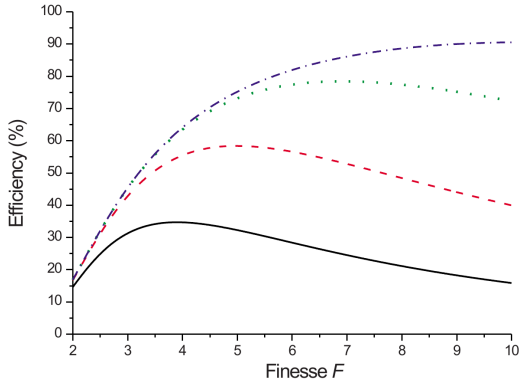

Figure 3.7: Efficency versus AFC finesse F for optical depth $d = 5$ (black solid line), $d = 10$ (red dashed line), $d = 20$ (green dotted line) and $d = 40$ (blue dashed-dotted line). This graph is plotted based on Eq.3.20. Image courtesy of ref.[5]

Figure.3.8 shows the efficiency in terms of optical depth.

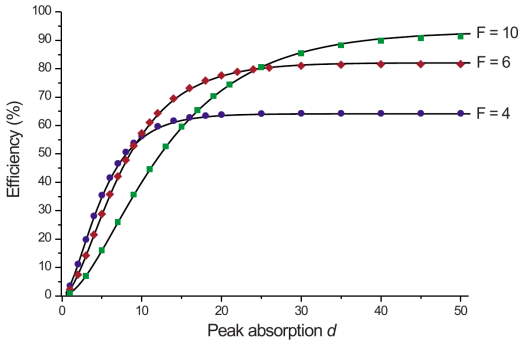

Figure 3.8: Memory efficency as a function of optical depth d for different AFC finesse values F. Solid lines are the result of analytical calculation Eq.3.20 and symbols are the result of numerical calculations. Image courtesy of ref.[5]

For each graph, the efficiency saturates with increasing optical depth, because of the dephasing due to the finite width of the peaks. The maximum achievable efficiency can be increased by using an AFC with a higher finesse, which has the cost of requiring more optical depth. One advantage of AFC compared to CRIB is that we remove fewer atoms through optical pumping, which increases the optical depth of system. Therefore we can achieve higher memory efficiency in the AFC. The

other advantage of AFC is its large mode capacity of storage due to the wide range of spectral coverage in this protocol.

AFC shares some features with photon echo with an accumulated grating in the absorption line, discovered in late 1970s [37]. Storage at the single-photon level with AFC was first demonstrated in 2008 [38]. In this work, light is stored light in Nd^{+3} ions doped into a YVO_4 crystal with a storage time of $250ns$, which is predetermined by the spacing in the comb structure and an efficiency of 0.5% in the forward direction. The same group performed on-demand storage by transferring atomic population to the auxiliary ground state using π-pulses [39]. Storage times of up to $20\mu s$ were achieved in praseodymium doped Y_2SiO_5 crystals with this method.

Chapter 4

Quantum Storage and Retrieval by Sweeping the Atomic Frequency

4.1 Scheme

Atom-photon interaction can be manipulated by several methods including using a control field in three-level atoms [8][9][10][11], photon echo technique [5] [14] [15], controlling the transition dipole moment of atoms [16], modulating the refractive index of the host medium of atoms [17]. Here we introduce manipulation of atom-photon interaction by means of changing the detuning between the atoms and the photons. By changing the energy level of the atoms we can sweep the bandwidth of the pulse and eventually absorb it into the atomic coherence. Thus the pulse must fit inside the medium in order for it to see all the swept frequencies.

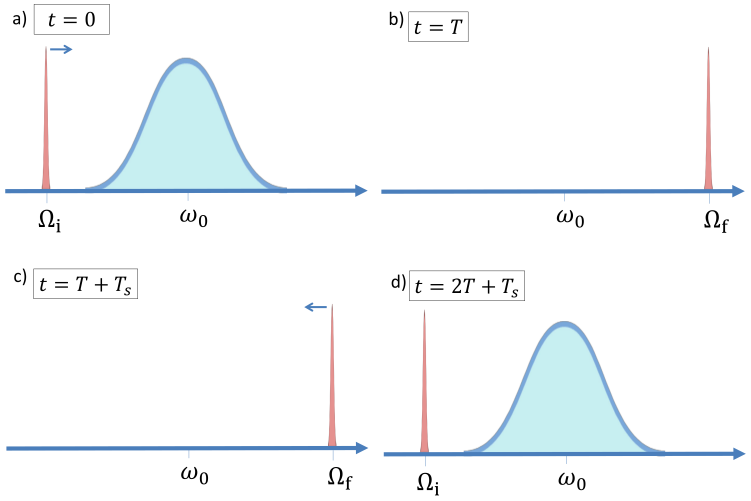

Figure 4.1: Scheme of atomic frequency change protocol. a) We start by changing the energy level of the atoms from lower than the energy of a photon ($\hbar\Omega_i$) and eventually, by changing the detuning to an energy level higher than the energy of a photon ($\hbar\Omega_f$) we can absorb the photon (b). We can have a photon stored in the atomic coherence for a storage time of T_s and then, by sweeping back the frequency of the atoms we can retrieve the photon(d)

4.2 Maxwell-Bloch Equations

We consider an ensemble of two level atoms interacting with a quantum field, which can be described with the dimensionless operator

$$\hat{E}(z,t) = \int d\omega \hat{a}_\omega(t) e^{ikz} + c.c. \tag{4.1}$$

To describe the quantum properties of the medium, we introduce the collective polarization operator i.e. average of polarization of atoms in the small but macroscopic volume containing $N_z \gg 1$ particles at position z [2]

$$\hat{P}(z,t) = \frac{d}{N_z} \sum_{j=1}^{N_z} \hat{\sigma}_{ge}^j n(z) \tag{4.2}$$

where $\hat{\sigma}_{\alpha\beta}^j = |\alpha_j\rangle\langle\beta_j|$ is the matrix element of the polarization of the j^{th} atom, $d = d_{ab} = d_{ba} = e\langle a|\vec{r}|a\rangle$ is the dipole moment of the atom, and $n(z) = \frac{N}{V}$ is the atomic density.

The Hamiltonian of such a system in the rotating wave approximation and dipole approximation is written as

$$\mathscr{H} = \int \hbar\omega \hat{a}_\omega \hat{a}_\omega^\dagger d\omega + \sum_{j=1}^{N} \hbar\Omega(t)\hat{\sigma}_{ee}^j - \hbar g \sum_{j=1}^{N} \int (\hat{a}_\omega e^{ikz_j} \hat{\sigma}_{eg}^j + H.C.) d\omega \tag{4.3}$$

where $\Omega(t)$ is the time dependent energy level of atoms, $g = \frac{d\cdot\varepsilon_k\hat{\varepsilon}}{\hbar}$ is the coupling constant between atoms and photons and $\varepsilon_k = \sqrt{\frac{\hbar\omega_0}{2\varepsilon_0 V}}$ is the electrical field per volume

4.2.1 Field Equation

We use slowly varying approximation by introducing slowly varying operators $\hat{\mathscr{E}}(z,t)$ and $\hat{\mathscr{P}}(z,t)$

$$\hat{E}(z,t) = \hat{\mathscr{E}}(z,t) e^{i(k_0 z - \omega_0 t)} + c.c. \tag{4.4}$$

$$\hat{P}(z,t) = \hat{\mathscr{P}}(z,t) e^{i(k_0 z - \omega_0 t)} + c.c. \tag{4.5}$$

where ω_0 and k_0 are the central frequency and wave vector of the input pulse respectively. Considering the slowly varying conditions

$$\begin{pmatrix} \partial_z \\ \partial_t \end{pmatrix} (\mathscr{E}, \mathscr{P}) \ll \begin{pmatrix} k_0 \\ \omega_0 \end{pmatrix} (\mathscr{E}, \mathscr{P}) \tag{4.6}$$

we obtain the wave equation

$$(\frac{\partial}{\partial z} + \frac{k_0}{\omega_0}\frac{\partial}{\partial t})\hat{\mathscr{E}} = \frac{i\omega_0^2}{2\varepsilon_k \varepsilon_0 k_0 c^2}\hat{\mathscr{P}} \tag{4.7}$$

We can substitute for $\hat{\mathscr{P}}$ from Eq.4.2 and Eq.4.5:

$$(c\frac{\partial}{\partial_z} + \frac{\partial}{\partial_t})\hat{\mathscr{E}} = igN\frac{1}{N_z}\hat{\sum}_{j=1}^{N_z}\sigma_{ge}^j e^{i(\omega_0 t - k_0 z)} \tag{4.8}$$

Now we define the collective operators:

$$\hat{\sigma}_{ee} = \frac{1}{N_z}\sum_{j=1}^{N_z}\hat{\sigma}_{ee}^j \tag{4.9}$$

$$\hat{\sigma}_{gg} = \frac{1}{N_z}\sum_{j=1}^{N_z}\hat{\sigma}_{gg}^j \tag{4.10}$$

$$\hat{\sigma}_{ge} = \frac{1}{N_z}\sum_{j=1}^{N_z}\hat{\sigma}_{ge}^j e^{i(\omega_0 t - k_0 z)} \tag{4.11}$$

Introducing these collective operators leads to a simple equation of motion for the field

$$(c\frac{\partial}{\partial_z} + \frac{\partial}{\partial_t})\hat{\mathscr{E}} = igN\hat{\sigma}_{ge} \tag{4.12}$$

4.2.2 Bloch Equation

The atomic evolution is governed by the Heisenberg equation

$$\begin{aligned}\frac{d}{dt}\hat{\sigma}_{ge} &= \frac{i}{\hbar}[H,\hat{\sigma}_{ge}] + \frac{\partial}{\partial t}\hat{\sigma}_{ge} + \hat{F}_{ge} \\ &= \frac{i\Omega(t)}{N_z}\sum_{j=1}^{N_z}[\hat{\sigma}_{ee}^{j},\hat{\sigma}_{ge}^{j}]e^{i(\omega_0 t-k_0 z)} - \frac{ig}{N_z}\sum_{j=1}^{N_z}e^{i(\omega_0 t-k_0 z)}[\hat{\sigma}_{eg}^{j},\hat{\sigma}_{ge}^{j}]\int a_\omega e^{ikz_j}d\omega + i\omega_0\hat{\sigma}_{ge} + \hat{F}_{ge} \\ &= -i(\Omega(t)-\omega_0)\hat{\sigma}_{ge} - ige^{i(\omega_0 t-k_0 z)}\frac{1}{N_z}\sum_{j=1}^{N_z}(\hat{\sigma}_{ee}^{j}-\hat{\sigma}_{gg}^{j})\int a_\omega e^{ikz_j}d\omega + \hat{F}_{ge} \end{aligned} \tag{4.13}$$

where $\hat{F}_{ge}$ is Langevin noise. Since our time scale is far less than the decay time, we need not take decay into account. Considering Eq.4.1 and Eq.4.4 for electric field and the definition of collective operators in Eqs.4.9-4.11, we can rewrite Eq.4.13 as

$$\frac{\partial}{\partial_t}\hat{\sigma}_{ge} = -i\Delta(t)\hat{\sigma}_{ge} - ig(\hat{\sigma}_{ee}-\hat{\sigma}_{gg})\hat{\mathscr{E}} + \hat{F}_{ge} \tag{4.14}$$

where $\Delta(t) = \Omega(t) - \omega_0$. In the weak field regime, we are far from saturation, so we can assume that most of the population still remains in the ground state. In other words, $\langle\sigma_{ee}\rangle = 0$, $\langle\sigma_{gg}\rangle = 1$. Hereafter, we write the equations in terms of the single photon wavefunction of the electric field ($\mathscr{E} = \langle 0|\hat{\mathscr{E}}|\psi_i\rangle$) and the single excitation wavefunction of the atomic coherence ($\sigma_{ge} = \langle 0|\hat{\sigma}_{ge}|\psi_i\rangle$) instead of field and atomic coherence operators. With these considerations we will have the following Maxwell-Bloch equations for our scheme

$$(c\frac{\partial}{\partial_z} + \frac{\partial}{\partial_t})\mathscr{E} = igN\sigma_{ge} \tag{4.15}$$

$$\frac{\partial}{\partial_t}\sigma_{ge} = -i\Delta(t)\sigma_{ge} + ig\mathscr{E} \tag{4.16}$$

Note that $\langle 0|\hat{F}_{ge}|\psi_i\rangle = 0$.

Thus far we have obtained the Maxwell-Bloch equations for our proposed scheme. In the next section we solve our obtained Maxwell-Bloch equations by paying attention to the eigen modes of the system, which is similar to the method called the polaritonic picture in EIT.

4.3 Polaritonic Description

This scheme also can be described by the so called polaritonic picture. We can write Eq.4.15 and Eq.4.16 in k-space as

$$\frac{\partial}{\partial t}\begin{pmatrix}\varepsilon(k,t)\\ \sigma_{ge}(k,t)\end{pmatrix} = i\begin{pmatrix}-kc & \beta\\ \beta & -\Delta(t)\end{pmatrix}\begin{pmatrix}\varepsilon(k,t)\\ \sigma_{ge}(k,t)\end{pmatrix} \tag{4.17}$$

One can solve this equation by looking at the eigen modes of the above set of equations i.e. mixtures of field and atomic coherences:

$$\Psi(k,t) = \cos\theta\varepsilon(k,t) + \sin\theta\sigma_{ge}(k,t) \tag{4.18}$$

$$\Phi(k,t) = -\sin\theta\varepsilon(k,t) + \cos\theta\sigma_{ge}(k,t) \tag{4.19}$$

where the mixing angle θ is given by

$$\sin 2\theta = \frac{2\beta^2}{\sqrt{4\beta^2+(ck+\Delta)^2}} \tag{4.20}$$

$$\cos 2\theta = \frac{-(ck+\Delta)}{\sqrt{4\beta^2+(ck+\Delta)^2}} \tag{4.21}$$

Considering the eigen modes of the system, the equations of motion become

$$\frac{\partial\Psi(k,t)}{\partial t} - i\lambda_1\Psi(k,t) = \dot{\theta}\Phi(k,t) \tag{4.22}$$

$$\frac{\partial\Phi(k,t)}{\partial t} - i\lambda_2\Phi(k,t) = \dot{\theta}\Psi(k,t) \tag{4.23}$$

where λ_1 and λ_2 are the eigen values of the system and $\dot{\theta}$ is the time derivative of the mixing angle:

$$\lambda_1 = \beta \cot\theta \tag{4.24}$$

$$\lambda_2 = -\beta \tan\theta \tag{4.25}$$

$$\dot{\theta} = -\frac{\dot{\Delta}}{4\beta^2}\sin^2 2\theta \tag{4.26}$$

Assuming $\dot{\Delta} \ll \beta^2$ we can neglect $\dot{\theta}$ compared to λ_1 in Eq.4.22 so that the eigen modes become decoupled. Now we Taylor expand the eigen values in terms of k, obtaining

$$\begin{aligned}
\lambda_1(k) &= \lambda_1(k=0) + \frac{\partial\lambda_1}{\partial k}\,|_{k=0}\,k + \frac{\partial^2\lambda_1}{\partial k^2}\,|_{k=0}\,k^2 + ... && (4.27)\\
&= \lambda_1(0) - c\cos^2\theta\, k + \frac{c^2}{4\beta}\sin^3 2\theta\, k^2 + ... && (4.28)
\end{aligned}$$

$$\begin{aligned}
\lambda_2(k) &= \lambda_2(k=0) + \frac{\partial\lambda_2}{\partial k}\,|_{k=0}\,k + \frac{\partial^2\lambda_2}{\partial k^2}\,|_{k=0}\,k^2 + ... && (4.29)\\
&= \lambda_2(0) - c\sin^2\theta\, k - \frac{c^2}{4\beta}\sin^3 2\theta\, k^2 + ... && (4.30)
\end{aligned}$$

In the regime where $\beta \gg \Delta\omega$, we can keep terms up to first order in k and neglect higher orders of k. With that, by transforming the equations back to z space we find the equations of motion for the eigen modes in real space:

$$\frac{\partial\Psi(z,t)}{\partial t} + c\cos^2\theta\frac{\partial\Psi(z,t)}{\partial z} = i\lambda_1(0)\Psi(z,t) \tag{4.31}$$

$$\frac{\partial\Phi(z,t)}{\partial t} + c\sin^2\theta\frac{\partial\Phi(z,t)}{\partial z} = i\lambda_2(0)\Phi(z,t) \tag{4.32}$$

Eq.4.31 and Eq.4.32 indicate that polaritons Ψ and Φ travel with group velocity $v_g = c\cos^2\theta$ and $v_g = c\sin^2\theta$ respectively. Figure.4.2 shows how the mixing angle θ varies with the detuning Δ.

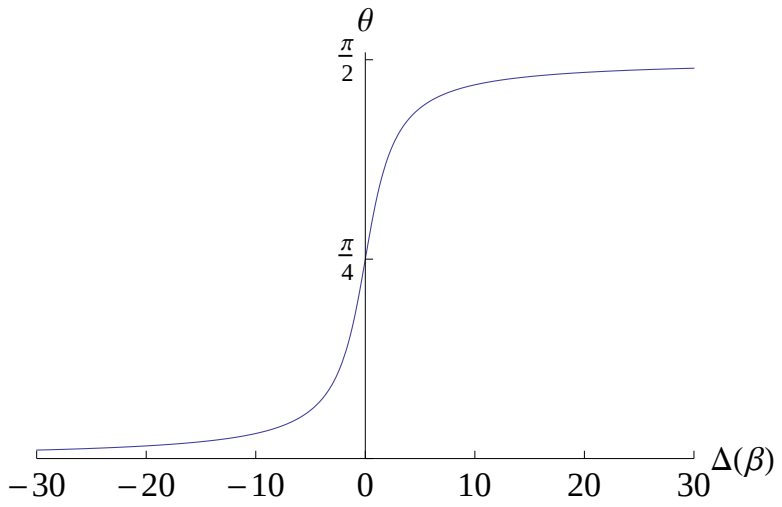

Figure 4.2: Mixed angle of θ as a function of detuning

Therefore if we start from a large negative (positive) detuning $-\Delta_0$ ($+\Delta_0$) compared to the coupling, we can couple the input pulse to the polariton Ψ (Φ) and by sweeping the detuning adiabatically to a large positive (negative) $+\Delta_0$ ($-\Delta_0$), we can slow the light and convert it to the atomic coherence reversibly.

4.4 Numerical Calculation

We have performed numerical simulations using 4-order Runge-Kutta method that is in agreement with the polaritonic picture described in the previous section. Figures.4.3(a),4.3(b) are simulation of the original Maxwell-Bloch equations Eq.4.15, Eq.4.16

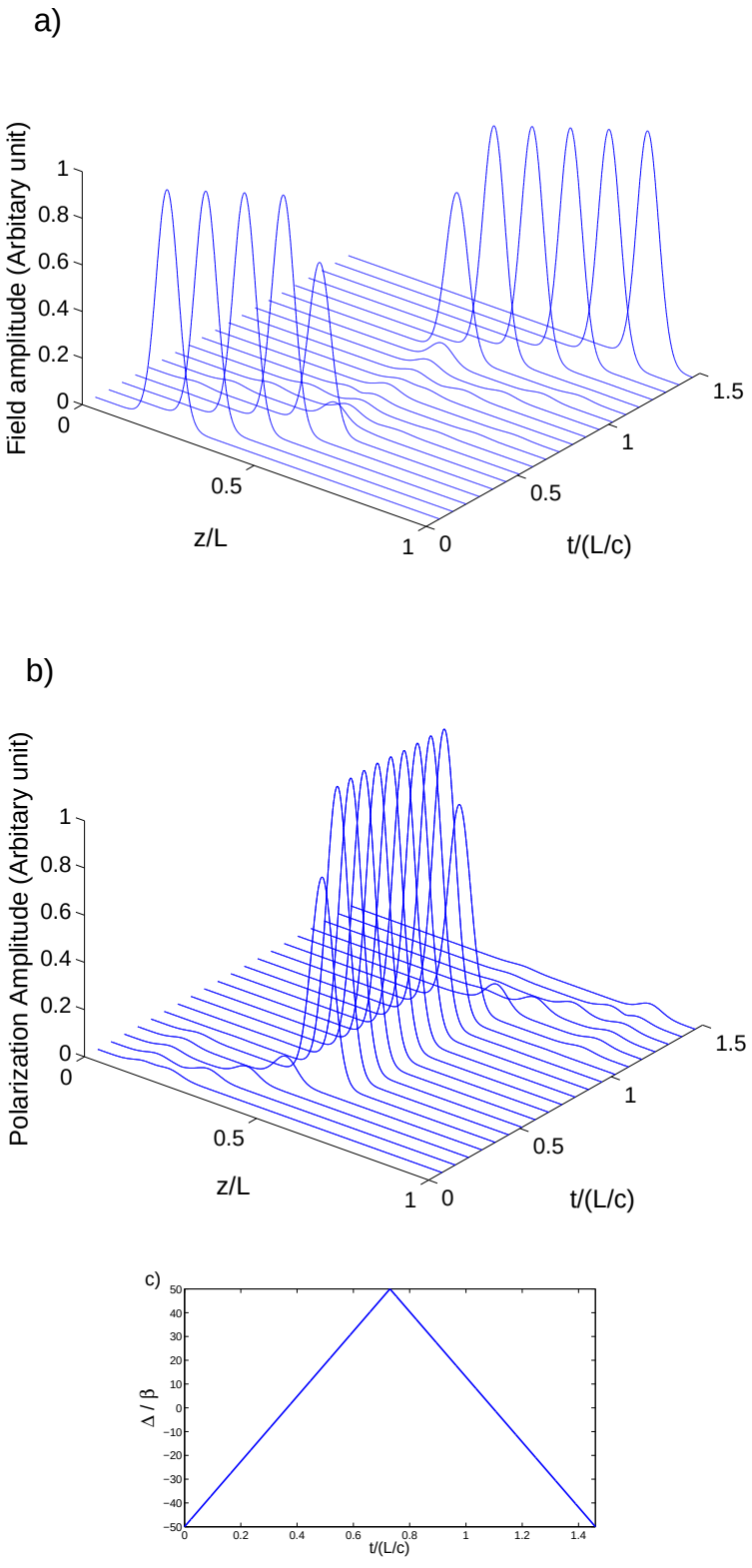

Figure 4.3: Propagation of field (a) and polarization (b) in the medium in time and space. (c) Detuning as a function of time, We start from $\Delta_0 = -50\beta$ and end to $+\Delta_0 = 50\beta$ with the rate of $\dot{\Delta} = 0.4\beta^2$. Coupling constant is set to $\beta = 30\Delta\omega$. The initial envelope is $exp-(z/z_0)^2$ where z_0 is $0.045L/c$

In addition we have compared the group velocity obtained from numerical calculations with the group velocity found in the polaritonic picture. Figure.4.4 shows the agreement between the numerical and analytical group velocities.

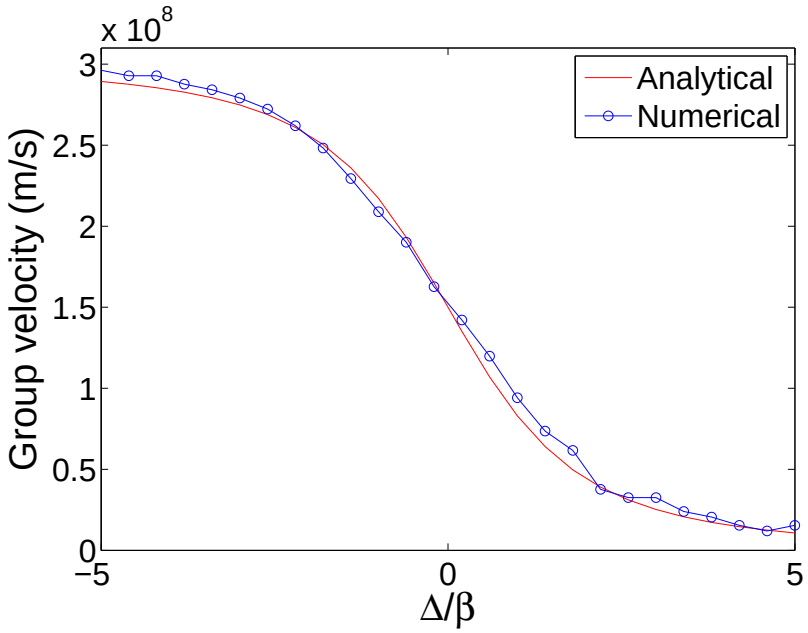

Figure 4.4: Comparison between group velocities resulting from analytical (red) and numerical (blue) calculations

Thus far we have assumed three conditions for storing light in one of the polaritons, which we restate together here:

$$\beta \ll \Delta_0 \tag{4.33}$$

$$\dot{\Delta} \ll \beta^2 \tag{4.34}$$

$$\Delta\omega \ll \beta \tag{4.35}$$

Now we study the importance of each of these conditions. First we examine condition 4.33. Figures.4.5(a)-4.5(g) show what happens when the condition 4.33 is violated.

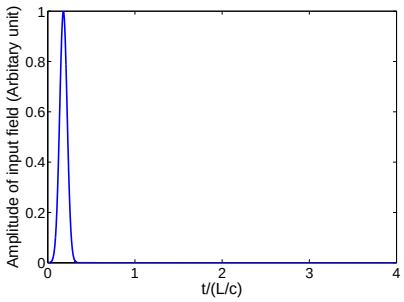

(a)

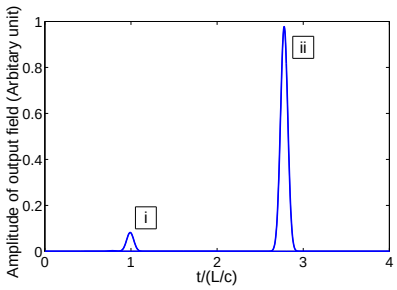

(b)

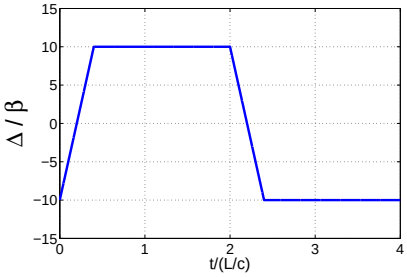

(c)

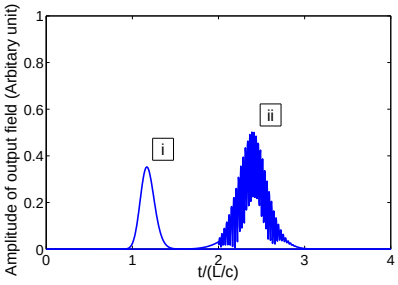

(d)

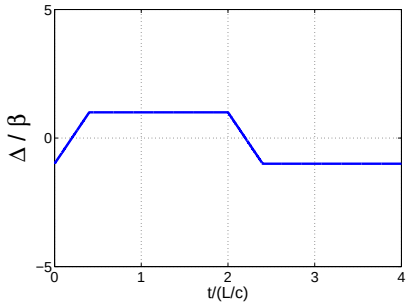

(e)

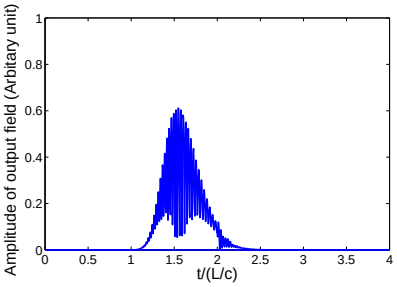

(f)

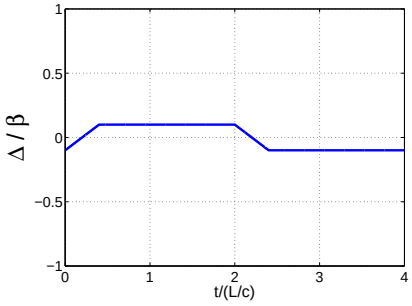

(g)

Figure 4.5: Effect of initial detuning on the output of the memory. The bandwidth of the input field is set to $\Delta\omega = 0.1\beta$. (a) shows the temporal shape of the input pulse. Note that the input pulse is initially in the medium . We sketch the output field for different values of initial detuning b)$\Delta_0 = -10\beta$, d)$\Delta_0 = -\beta$, f)$\Delta_0 = -0.1\beta$. (c), (e), (g) show how detuning changes in each case. (i) is transmitted and (ii) is retrieved pulse.

It can be seen that by decreasing the initial detuning (while the other conditions are fulfilled), we excite polariton Φ (i) more and polariton Ψ (ii) become less excited. According to Eq.4.31 and Eq.4.32, as we change the detuning, polariton Ψ slows down and converts to polarization while polariton Φ accelerates from zero group velocity to speed of light and leaves the medium. Therefore excitement of polariton Φ is considered to be loss in this protocol. When the starting detuning is much less than the coupling rate (Figure.4.5(f)), θ is almost $\pi/4$ so according to Eq.4.31 and Eq.4.32 both polaritons travel with speed $c/2$ and, since they have opposite phase ($\lambda_1 = \beta$ and $\lambda_2 = -\beta$), they undergo a series of reemission and absorption processes with rate β (Figure.4.5(d) and Figure.4.5(f))

Secondly we examine the adiabaticity condition 4.34. Figures.4.6(a)-4.6(g) show that how the output field changes when we violate adiabaticity condition.

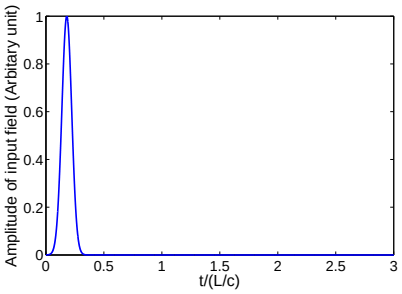

(a)

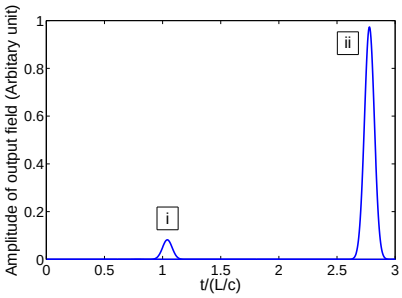

(b)

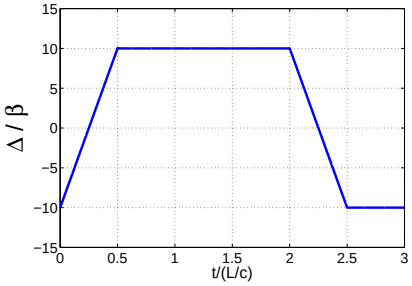

(c)

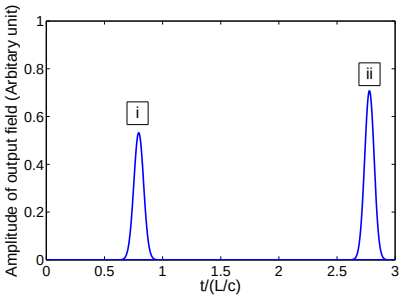

(d)

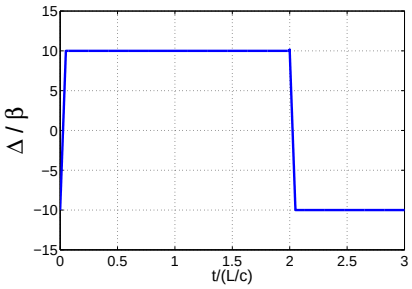

(e)

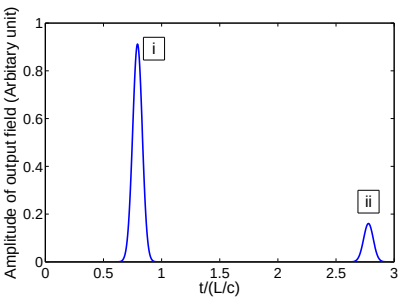

(f)

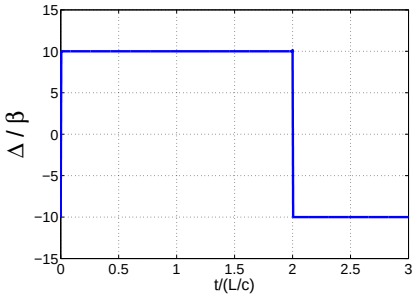

(g)

Figure 4.6: Effect of the rate of changing the detuning on the output of the memory. The bandwidth of the input field is set to $\Delta\omega = 0.1\beta$. (a) shows the temporal shape of the input pulse. Note that the input pulse is initially in the medium. The initial detuning for all of the cases is $\Delta_0 = -10\beta$. We sketch the output field for different values of $\dot{\Delta}$, b)$\dot{\Delta} = 0.3\beta^2$, d)$\dot{\Delta} = 3\beta^2$, f)$\dot{\Delta} = 30\beta^2$. (c), (e), g are detuning as a function of time. (i) is transmitted and (ii) is retrieved pulse.

As we increase $\dot{\Delta}$ (while the other two conditions hold), the process becomes less adiabatic, resulting in leakage of polariton Ψ (ii) into the polariton Φ (i) which accelerates to the speed of light and leaves the medium. Therefore this condition is necessary for efficient absorption of the light.

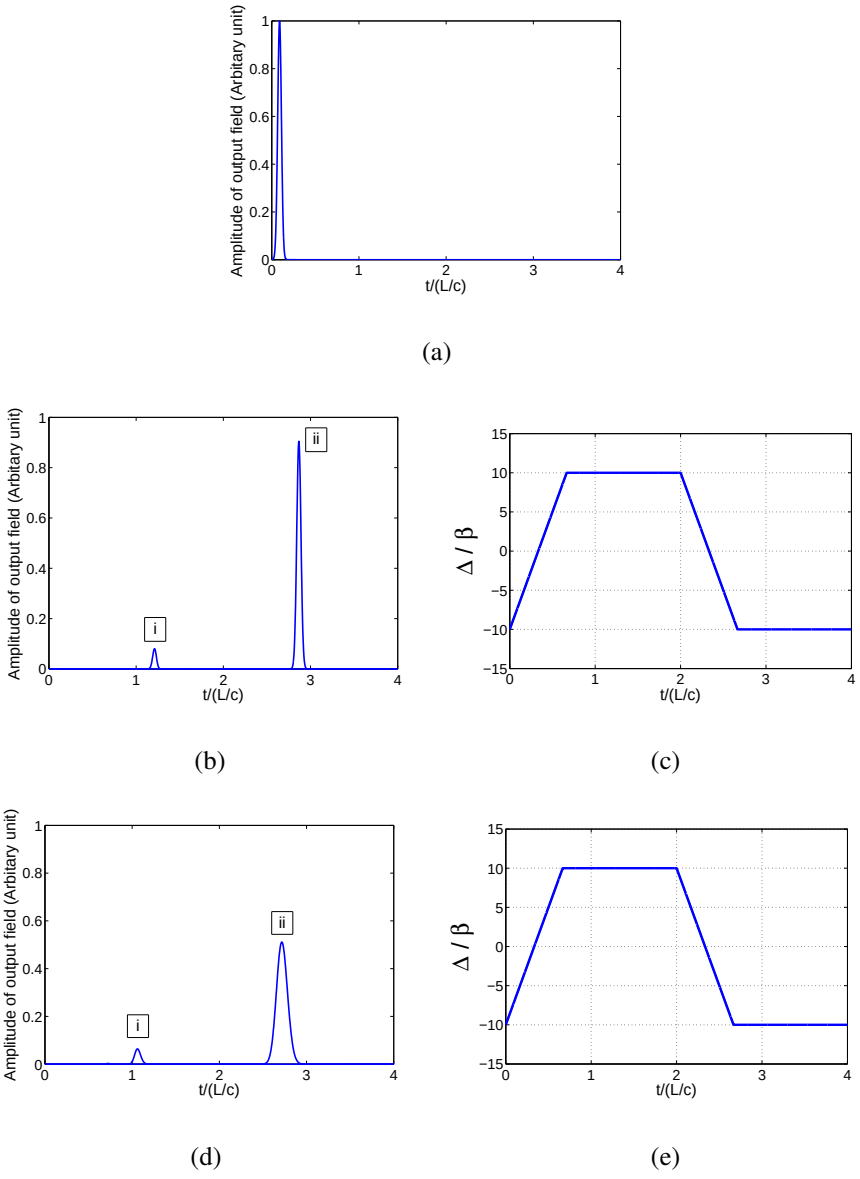

Figure 4.7: Effect of the value of β (compared to the bandwidth of the input pulse) on output of the memory. (a) shows the temporal shape of the input pulse. Note that the input pulse is initially in the medium. Initial detuning for all of the cases is $\Delta_0 = -10\beta$. We sketch the output field for two different values of β b) $\beta = 16\Delta\omega$, d)$\beta = 4\Delta\omega$. (c), (e) are the detuning as a function of time. (i) is transmitted and (ii) is retrieved pulse.

Finally we study the effect of violating condition 4.35. Figures.4.7(a)-4.7(e) show how the output changes when the coupling rate approaches the bandwidth of the pulse.

It can be seen that when β approaches the bandwidth, the output pulse becomes broader, which reduces the fidelity of the memory protocol. This can be explained by considering the expansion of the eigen values in terms of k in Eq.4.28. When β is comparable to the bandwidth of the pulse, we no longer can neglect second and higher orders of k in Eqs.4.28 and 4.30, resulting in dispersion of the pulse.

4.5 Experimental Requirements

As we mentioned earlier in order to store the pulse efficiently, the pulse has to be fit inside the medium, otherwise frequency components of the pulse that were not in the medium at the time that atoms had the corresponding frequency, don't become absorbed in the medium. This imposes a condition on the frequency bandwidth of the input pulses ($\Delta\omega \gg \frac{c}{L}$). This condition along with the requirement for avoiding dispersion of the pulse in the medium Eq.4.35 ($\beta \gg \Delta\omega$) requires demanding optical depth for the medium

$$d = \frac{\beta^2 L}{c\gamma} \gg \frac{\beta}{\gamma} \tag{4.36}$$

where γ is the decay rate. For having high efficiency, decay rate should be smaller than the bandwidth of the pulse ($\gamma \ll \Delta\omega$) and as we mentioned earlier for having high fidelity, coupling constant should be larger than the bandwidth of the pulse ($\beta \gg \Delta\omega$). Therefore coupling constant should be at least two order of magnitude larger than decay rate. This condition implies that optical depth (Eq.4.36) requires to be of the order of thousand to store the photon with high efficiency and fidelity. It is worth mentioning that the same condition on the optical depth can be obtained by using adiabaticity condition Eq.4.34 and initial detuning requirement Eq.4.33.

The other challenge for implementation of atomic frequency change memory is the range that atomic frequency has to be swept. As we discussed earlier (Eq.4.33) to avoid mixing eigen modes

of the system, the range of swept atomic frequency should be larger than coupling constant ($\Delta_0 \gg \beta$) which demands a two level system with isolation of more than three orders of magnitude larger than linewidth.

Chapter 5

Connection to Gradient Echo Memory (GEM)

Intuitively atomic frequency change protocol is similar to the Gradient Echo Memory (GEM) protocol for the regime in which pulses are short compared to the length of the medium. While we change the detuning in time during the propagation of the pulse through the medium, the pulse effectively sees a spatial gradient in the energy level of the atoms and the atomic coherence becomes dephased.

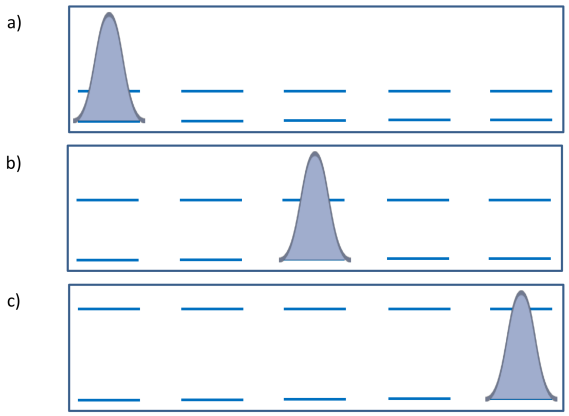

Figure 5.1: Pulse experiences effective spatial gradient while atomic frequency changes in time

This fact can be captured rigorously by transforming the equations of motions 4.15, 4.16 to the retarded frame ($\tau \to t - z/c$, $z' = z$):

$$\frac{\partial}{\partial \tau}\sigma_{ge}(\tau,z) = -i\Delta(\tau+\frac{z}{c})\sigma_{ge}(\tau,z) + i\beta\mathscr{E}(\tau,z) \tag{5.1}$$

$$\frac{\partial}{\partial z}\mathscr{E}(\tau,z) = \frac{i\beta}{c}\sigma_{ge}(\tau,z) \tag{5.2}$$

Note that this set of equations is nonlocal, However with the approximation that we make in the following, they become local equations. For pulses smaller than the medium, since the range

of τ most of the time is of the same order of magnitude as the time duration of the pulse and $\frac{z}{c}$ is of the same order of magnitude as $\frac{L}{c}$, term τ can be neglected compared to $\frac{z}{c}$. As a result we end up with GEM equations

$$\frac{\partial}{\partial \tau}\sigma_{ge}(\tau,z) = -i\dot{\Delta}\frac{z}{c}\sigma_{ge}(\tau,z) + i\beta\mathscr{E}(\tau,z) \tag{5.3}$$

$$\frac{\partial}{\partial z}\mathscr{E}(\tau,z) = \frac{i\beta}{c}\sigma_{ge}(\tau,z) \tag{5.4}$$

Here, $\frac{\dot{\Delta}}{c}$ is the term corresponding to the spatial gradient term (χ) in GEM ([15]) . Note that this set of equations is no longer non-local and has been solved for the case of the GEM memory [15]. By following a similar analysis the effective optical depth is found to:

$$d_e = \frac{\beta^2}{\dot{\Delta}} \tag{5.5}$$

For high efficiency, the effective optical depth must be larger than one ($d_e > 1$), which leads to an upper bound for the rate of change of the detuning,

$$\dot{\Delta} < \beta^2 \tag{5.6}$$

It is remarkable that the optical depth requirement exactly matches the adiabaticity condition that we obtained for the the atomic frequency change memory. It suggests that the optical depth requirement can be interpreted as leakage of the pulse into a mode which travels at the speed of light. We have also performed the numerical comparisons between the GEM and atomic frequency change memory whose effective spatial gradient ($\frac{\dot{\Delta}}{c}$) is equal to the spatial gradient in GEM (χ)

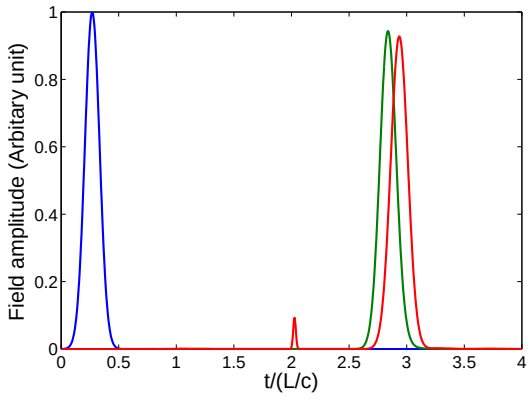

(a)

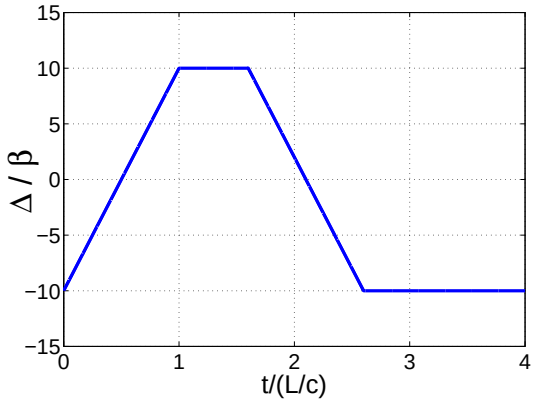

(b)

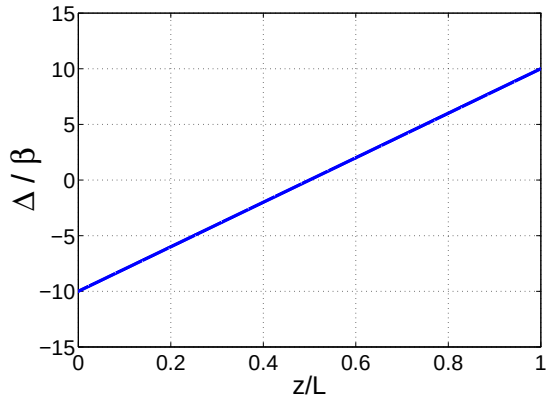

(c)

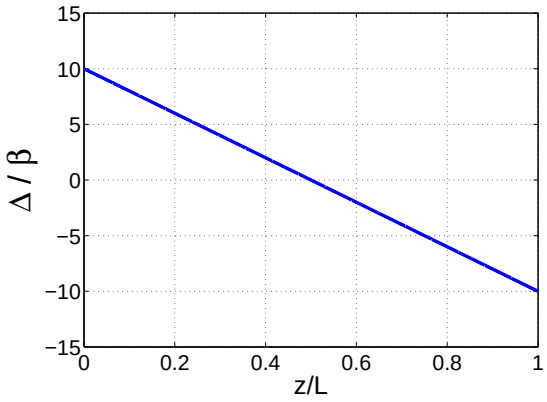

(d)

Figure 5.2: (a) Comparison of the atomic frequency change memory output (green) with GEM output (red) when we send the same input pulse (blue). (b) illustrates the detuning as a function of time. The detuning as a function of time during the (c) storage and (d) retrieval. In the simulation of the GEM, at time t=1.6L/c energy level of atoms are flipped. Spatial gradient ($\frac{\dot{A}}{c}$) in atomic frequency change memory in both storage and retrieval is set to the spatial gradient in GEM (χ).

Figure.5.2 shows the agreement between outputs of the two protocols. It is important to note that Eqs.(5.3) and (5.4) were derived with the assumption that retarded time is much smaller than the temporal extension of medium (L/c) which is true for the short pulses traveling with almost the speed of light. However based on polaritonic description (Chapter 4) we know that the pulse slows down in the medium, and as a result the retarded time increases more than the time duration of the pulse and our assumption is no longer valid. What justifies our approximation is that, when the retarded time exceeds L/c, the pulse is almost absorbed. Thus this factor doesn't play an important role. The small discrepancy of the two protocols in the Figure.5 can be explained by this imperfection of approximation.

Chapter 6

Conclusion

We have presented a new protocol for quantum storage of light based on sweeping the atomic frequency. We have described this protocol by deriving a polaritonic picture and found the requirements for efficient storage of light with high fidelity. First of all the pulse should fit inside the medium in order to experience all of the swept frequency. For efficient storage we have to start with a detuning much larger than coupling constant ($\Delta_0 \gg \beta$) and sweep the atomic frequency while obeying the adiabatic condition $\dot{\Delta} \ll \beta^2$, otherwise our polaritonic mode of interest leaks to the other polaritonic mode that travels with the speed of light and escapes the medium. Also in order to avoid the dispersion of the pulse in the medium, the coupling constant should be larger than the spectral bandwidth of the pulse, $\beta \gg \Delta\omega$. We have verified the necessity of all of these conditions by numerical analysis. These conditions imply requirements of large optical depth requirement (of the order of a thousand) and large level separation (three orders of magnitude more than the linewidth).

In addition, we have shown the connection between atomic frequency change memory and GEM memory for short pulses by going to the co-moving frame, supported by both analytical and numerical calculations.

In conclusion we have proposed a quantum memory protocol which, on the one hand, shares lots of similarities with slow light quantum memories, and on the other hand, is similar to the GEM memory. It thus forms a bridge between two well known quantum memory protocols.

For the future, we are planning to study the experimental requirements in more detail. We will also further pursue the idea of a unification of quantum memory protocols.

Bibliography

[1] Alexander I. Lvovsky, Barry C. Sanders, and Wolfgang Tittel. Optical quantum memory. *Nature Photonics*, 3(12):706–714, December 2009.

[2] M. Fleischhauer and MD Lukin. Dark-state polaritons in electromagnetically induced transparency. *Physical Review Letters*, 84(22):5094–5097, 2000.

[3] W. Tittel, M. Afzelius, T. Chaneliere, R. L. Cone, S. Kroll, S. A. Moiseev, and M. Sellars. Photon-echo quantum memory in solid state systems. *Laser & Photonics Reviews*, 4(2):244–267, 2010.

[4] G. Hétet, J. J. Longdell, M. J. Sellars, P. K. Lam, and B. C. Buchler. Multimodal properties and dynamics of gradient echo quantum memory. *Phys. Rev. Lett.*, 101:203601, Nov 2008.

[5] Mikael Afzelius, Christoph Simon, Hugues de Riedmatten, and Nicolas Gisin. Multimode quantum memory based on atomic frequency combs. *Phys. Rev. A*, 79:052329, May 2009.

[6] Klemens Hammerer, Anders S. Sørensen, and Eugene S. Polzik. Quantum interface between light and atomic ensembles. *Rev. Mod. Phys.*, 82:1041–1093, Apr 2010.

[7] C. Simon, M. Afzelius, J. Appel, A. B. de la Giroday, S. J. Dewhurst, N. Gisin, C. Y. Hu, F. Jelezko, S. Kroll, J. H. Muller, J. Nunn, E. S. Polzik, J. G. Rarity, H. De Riedmatten, W. Rosenfeld, A. J. Shields, N. Skold, R. M. Stevenson, R. Thew, I. A. Walmsley, M. C. Weber, H. Weinfurter, J. Wrachtrup, and R. J. Young. Quantum memories. *European Physical Journal D*, 58(1):1–22, 2010.

[8] M. Fleischhauer and M. D. Lukin. Quantum memory for photons: Dark-state polaritons. *Phys. Rev. A*, 65:022314, Jan 2002.

[9] J. Nunn, I. A. Walmsley, M. G. Raymer, K. Surmacz, F. C. Waldermann, Z. Wang, and

D. Jaksch. Mapping broadband single-photon wave packets into an atomic memory. *Phys. Rev. A*, 75:011401, Jan 2007.

[10] Alexey V. Gorshkov, Axel André, Michael Fleischhauer, Anders S. Sørensen, and Mikhail D. Lukin. Universal approach to optimal photon storage in atomic media. *Phys. Rev. Lett.*, 98:123601, Mar 2007.

[11] K. F. Reim, J. Nunn, V. O. Lorenz, B. J. Sussman, K. C. Lee, N. K. Langford, D. Jaksch, and I. A. Walmsley. Towards high-speed optical quantum memories. *Nature Photonics*, 4(4):218–221, March 2010.

[12] U.G. Kopvil'em and V.R. Nagibarov. *Fiz. Metall.Metalloved*, 2:313, 1963.

[13] N. A. Kurnit, I. D. Abella, and S. R. Hartmann. Observation of a photon echo. *Phys. Rev. Lett.*, 13:567–568, Nov 1964.

[14] Nicolas Sangouard, Christoph Simon, Mikael Afzelius, and Nicolas Gisin. Analysis of a quantum memory for photons based on controlled reversible inhomogeneous broadening. *Phys. Rev. A*, 75:032327, Mar 2007.

[15] J. J. Longdell, G. Hétet, P. K. Lam, and M. J. Sellars. Analytic treatment of controlled reversible inhomogeneous broadening quantum memories for light using two-level atoms. *Phys. Rev. A*, 78:032337, Sep 2008.

[16] Khabat Heshami, Adam Green, Yang Han, Arnaud Rispe, Erhan Saglamyurek, Neil Sinclair, Wolfgang Tittel, and Christoph Simon. Controllable-dipole quantum memory. *Phys. Rev. A*, 86:013813, Jul 2012.

[17] James Clark, Khabat Heshami, and Christoph Simon. Photonic quantum memory in two-level ensembles based on modulating the refractive index in time: Equivalence to gradient echo memory. *Phys. Rev. A*, 86:013833, Jul 2012.

[18] Lene V. Hau, S. E. Harris, Zachary Dutton, and Cyrus H. Behroozi. Light speed reduction to 17 metres per second in an ultracold atomic gas. *Nature*, 397(6720):594–598, February 1999.

[19] Marlan O. Scully and M. Suhail Zubairy. *Quantum Optics*. Cambridge University Press, 1 edition, September 1997.

[20] Michael Fleischhauer and Aaron S. Manka. Propagation of laser pulses and coherent population transfer in dissipative three-level systems: An adiabatic dressed-state picture. *Phys. Rev. A*, 54:794–803, Jul 1996.

[21] D. F. Phillips, A. Fleischhauer, A. Mair, R. L. Walsworth, and M. D. Lukin. Storage of light in atomic vapor. *Phys. Rev. Lett.*, 86:783–786, Jan 2001.

[22] Chien Liu, Zachary Dutton, Cyrus H. Behroozi, and Lene V. Hau. Observation of coherent optical information storage in an atomic medium using halted light pulses. *Nature*, 409(6819):490–493, January 2001.

[23] J. J. Longdell, E. Fraval, M. J. Sellars, and N. B. Manson. Stopped light with storage times greater than one second using electromagnetically induced transparency in a solid. *Phys. Rev. Lett.*, 95:063601, Aug 2005.

[24] T. Chanelière, D.N. Matsukevich, S.D. Jenkins, S.-Y. Lan, T.A.B. Kennedy, and A. Kuzmich. Storage and retrieval of single photons transmitted between remote quantum memories. *Nature*, 438(7069):833–836, 2005.

[25] M. D. Eisaman, A. André, F. Massou, M. Fleischhauer, A. S. Zibrov, and M. D. Lukin. Electromagnetically induced transparency with tunable single-photon pulses. *Nature*, 438(7069):837–841, December 2005.

[26] Irina Novikova, Alexey V. Gorshkov, David F. Phillips, Anders S. Sørensen, Mikhail D.

Lukin, and Ronald L. Walsworth. Optimal control of light pulse storage and retrieval. *Phys. Rev. Lett.*, 98:243602, Jun 2007.

[27] Jürgen Appel, Eden Figueroa, Dmitry Korystov, M. Lobino, and A. I. Lvovsky. Quantum memory for squeezed light. *Phys. Rev. Lett.*, 100:093602, Mar 2008.

[28] E. L. Hahn. Spin echoes. *Phys. Rev.*, 80:580–594, Nov 1950.

[29] S.O. Elyutin, S.M Zakharov, and E.A. Manykin. *Sov.Phys.JETP*, 49:421, 1979.

[30] T.W. Mossberg. Time-domain frequency-selective optical data storage. *Opt. Lett.*, 7:77–79, 1982.

[31] H. Lin, T. Wang, and T. W. Mossberg. Demonstration of 8-gbit/in.2 areal storage density based on swept-carrier frequency-selective optical memory. *Opt. Lett.*, 20(15):1658–1660, Aug 1995.

[32] Jérôme Ruggiero, Jean-Louis Le Gouët, Christoph Simon, and Thierry Chanelière. Why the two-pulse photon echo is not a good quantum memory protocol. *Phys. Rev. A*, 79:053851, May 2009.

[33] S. A. Moiseev and S. Kröll. Complete reconstruction of the quantum state of a single-photon wave packet absorbed by a doppler-broadened transition. *Phys. Rev. Lett.*, 87:173601, Oct 2001.

[34] A. L. Alexander, J. J. Longdell, M. J. Sellars, and N. B. Manson. Photon echoes produced by switching electric fields. *Phys. Rev. Lett.*, 96:043602, Feb 2006.

[35] M. Hosseini, G. Campbell, B. M. Sparkes, P. K. Lam, and B. C. Buchler. Unconditional room-temperature quantum memory. *Nature Physics*, 7:794, Jun 2011.

[36] Morgan P. Hedges, Jevon J. Longdell, Yongmin Li, and Matthew J. Sellars. Efficient quantum memory for light. *Nature*, 465(7301):1052–1056, June 2010.

[37] Wim H. Hesselink and Douwe A. Wiersma. Picosecond photon echoes stimulated from an accumulated grating. *Phys. Rev. Lett.*, 43:1991–1994, Dec 1979.

[38] Hugues de Riedmatten, Mikael Afzelius, Matthias U. Staudt, Christoph Simon, and Nicolas Gisin. A solid-state lightmatter interface at the single-photon level. *Nature*, 456(7223):773–777, December 2008.

[39] Mikael Afzelius, Imam Usmani, Atia Amari, Björn Lauritzen, Andreas Walther, Christoph Simon, Nicolas Sangouard, Ji říMinář, Hugues de Riedmatten, Nicolas Gisin, and Stefan Kröll. Demonstration of atomic frequency comb memory for light with spin-wave storage. *Phys. Rev. Lett.*, 104:040503, Jan 2010.